

This discussion paper is/has been under review for the journal *Atmospheric Chemistry and Physics (ACP)*. Please refer to the corresponding final paper in *ACP* if available.

**Principal
components of
particle size
distributions**

F. Costabile et al.

Spatio-temporal variability and principal components of the particle number size distribution in an urban atmosphere

F. Costabile^{1,2}, W. Birmili¹, S. Klose¹, T. Tuch^{1,3}, B. Wehner¹, A. Wiedensohler¹, U. Franck³, K. König¹, and A. Sonntag¹

¹Leibniz Institute for Tropospheric Research, Leipzig, Germany

²C.N.R. – IIA, Via Salaria Km 29, 3, 00016 Monterotondo Scalo (Roma), Italy

³Helmholtz Center for Environmental Research, Leipzig, Germany

Received: 18 July 2008 – Accepted: 27 August 2008 – Published: 16 October 2008

Correspondence to: W. Birmili (birmili@tropos.de)

Published by Copernicus Publications on behalf of the European Geosciences Union.

Title Page

Abstract

Introduction

Conclusions

References

Tables

Figures

⏪

⏩

◀

▶

Back

Close

Full Screen / Esc

Printer-friendly Version

Interactive Discussion

Abstract

Due to the presence of diffusive anthropogenic sources in urban areas, the spatio-temporal variability of fine (diameter $<1\ \mu\text{m}$) and ultrafine ($<0.1\ \mu\text{m}$) aerosol particles has been a challenging issue in particle exposure assessment as well as atmospheric research in general. We examined number size distributions of atmospheric aerosol particles (size range 3–800 nm) that were measured simultaneously at a maximum of eight observation sites in and around a city in Central Europe (Leipzig, Germany). Two main experiments were conducted with different time span and number of observation sites (2 years at 3 sites; 1 month at 8 sites). A general observation was that the particle number size distribution varied in time and space in a complex fashion as a result of interaction between local and far-range sources, and the meteorological conditions. To identify statistically independent factors in the urban aerosol, different runs of principal component analysis were conducted encompassing aerosol, gas phase, and meteorological parameters from the multiple sites. Several of the resulting principal components, outstanding with respect to their temporal persistence and spatial coverage, could be associated with aerosol particle modes: a first accumulation mode (“droplet mode”, 300–800 nm), considered to be the result of liquid phase processes and far-range transport; a second accumulation mode (centered around diameters 90–250 nm), considered to result from primary emissions as well as aging through condensation and coagulation; an Aitken mode (30–200 nm) linked to urban traffic emissions in addition to an urban and a rural Aitken mode; a nucleation mode (5–20 nm) linked to urban traffic emissions; nucleation modes (3–20 nm) linked to photochemically induced particle formation; an aged nucleation mode (10–50 nm). A number of additional components were identified to represent only local sources at a single site each, or infrequent phenomena. In summary, the analysis of size distributions of high time and size resolution yielded a surprising wealth of statistical aerosol components occurring in the urban atmosphere over one single city. Meanwhile, satisfactory physical explanations could be found for the components with the greatest temporal persistence and spatial

ACPD

8, 18155–18217, 2008

Principal components of particle size distributions

F. Costabile et al.

Title Page

Abstract

Introduction

Conclusions

References

Tables

Figures

⏪

⏩

◀

▶

Back

Close

Full Screen / Esc

Printer-friendly Version

Interactive Discussion

coverage. Therefore a paradigm on the behaviour of sub- μm urban aerosol particles is proposed, with recommendations how to efficiently monitor individual sub-fractions across an entire city.

1 Introduction

5 Atmospheric aerosol particles have been acknowledged to play a key role with respect to the global balance of climate (Haywood and Boucher, 2000; Stott et al., 2000; Ramanathan et al., 2001). Several aerosol effects, including optical absorption, scattering and cloud-activation are more sensitive on total particle surface area and number than total particle mass. Understanding the properties and the life-cycle of the entire particle
10 size distribution is therefore required to assess aerosol-driven climate effects.

Besides climate, aerosol particles have been recognised as a potential adverse factor for human health (Pope et al., 2002; WHO, 2002; Oberdöster, 2005). While many of the health-related evidence has been based on PM_{10} mass concentrations as a particle
15 metric, specific questions have arisen which particular aerosol types might be responsible, and how the exposure risk for the population may be reduced in a cost-efficient way. Specific sub-groups in the environmental aerosol that are suspected to cause adverse health effects are, among others, carbonaceous aerosols, insoluble particles, traffic-related aerosols, metal aerosols, and ultrafine particles (diameter < 100 nm) (HEI,
20 2002). A current trend in air quality monitoring is to refine the measurement techniques and thus identify the abundance (and later the possible health effects) of these aerosol sub-fractions.

A frequent observation is that atmospheric aerosol particles occur in particle modes, i.e. populations of similar size and chemical composition. Modes manifest themselves by a peak in the physical or chemical particle size distribution. Whitby (1978) popularised the tri-modal scheme including the coarse, the accumulation, and the “nuclei”
25 (i.e. Aitken) mode, and this scheme has ever since been confirmed for different environments, refined and expanded (Ondov and Wexler, 1998; Mäkelä et al., 2000; Birmili

Principal components of particle size distributions

F. Costabile et al.

Title Page

Abstract

Introduction

Conclusions

References

Tables

Figures

⏪

⏩

◀

▶

Back

Close

Full Screen / Esc

Printer-friendly Version

Interactive Discussion



et al., 2001; Hussein et al., 2004; Heintzenberg et al., 2004; Morawska et al., 2008). In a remote background atmosphere these modes reflect the age and the life-time of the particles (Jaenicke, 1993), while in urban environments, they can reveal the proximity and/or activity of anthropogenic sources. Examples of tropospheric aerosol particle modes are the nucleation mode (Kulmala et al., 2004), the Aitken mode, the accumulation mode, the droplet mode resulting from liquid-phase processes (John, 1993), or the sea-spray mode in the coarse particle size range.

Being able to detect and describe aerosol particle modes can provide insight into the relevance of different aerosol sources and generation processes relevant in a particular section of the atmosphere. Knowledge on the spatio-temporal behaviour of aerosol modes could greatly simplify the description of aerosol-related processes and effects, and also particle exposure assessment. On the other hand, we always need to keep in mind the complex structure of the atmospheric aerosol - each single particle usually contains a different and complex mixture of chemical substances after a few days of residence in the atmosphere (Ebert et al., 2004), which means that any paradigm of particle modes can only be an approximation of the reality. The temporal and spatial variability of ambient aerosols has been the subject of many atmospheric studies. Sioutas et al. (2005) came to the conclusion that for ultrafine particles (UFPs; diameter <100 nm), measurements independent from total particle mass (PM_{10} , $PM_{2.5}$, and even PM_1) are needed to characterise their full impact on human health. While PM mass concentrations appear to be less variable in time and space, this is not true for particle number concentration, or the concentration of ultrafine particles.

Puustinen et al. (2007) studied in 4 European cities the correlation between ambient particle number and mass concentrations at a central site and a number of residential houses; their conclusion was that a central site measurement can be representative for a wide part of a city when referring to $PM_{2.5}$ and PM_{10} mass concentration, but not for particle number. Hussein et al. (2005) showed for three pairs of sites that the number of ultrafine particles were less correlated between the sites than the number of bigger particles (>100 nm). Tuch et al. (2006) showed that the inter-site correlation within a

Principal components of particle size distributions

F. Costabile et al.

Title Page

Abstract

Introduction

Conclusions

References

Tables

Figures



Back

Close

Full Screen / Esc

Printer-friendly Version

Interactive Discussion

city can go to values near zero when comparing UFP concentrations at sites whereof one site is traffic-influenced. In western cities, emissions from motor traffic are one of the main reasons for this lack of spatial correlations of UFPs (Ketzler et al., 2004; Bukowiecki et al., 2003).

5 A characterisation of the spatial distribution of exposure to ambient fine and ultrafine particles in a particular city requires, in any case, spatially-resolved UFP measurements and/or a coupled emission and transport modelling of UFPs across an urban landscape. Up to now, however, multiple-point measurements of UFPs have been scarce, time series limited, and dispersion models mainly been available for local micro environments, at rough spatial resolution, or without a treatment of ultrafine particle dynamics.

10 In this work, we studied the temporal and spatial variations of sub- μm particle size distributions across a city in Central Europe (Leipzig, Germany) with the aid of multiple-site observations. Specific effects of urban and regional particle sources as well as urban meteorology are illustrated. Principal component analysis (PCA) is used to statistically isolate the main source/meteorological factors governing the particle number size distribution (PNSD) observed at the ensemble of sites. Particular emphasis is directed towards the dependency of temporal and spatial variations on particle size, and the consequences of the observations on spatial particle exposure. The paper concludes with a general paradigm on the behaviour of sub- μm particle modes in the area under study, and a recommendation how to efficiently monitor these particle sub-fractions across an entire city.

2 Experimental

2.1 Field experiment and data

25 Two main resources of atmospheric aerosol particle size distributions were used for this work:

Principal components of particle size distributions

F. Costabile et al.

Title Page

Abstract

Introduction

Conclusions

References

Tables

Figures



Back

Close

Full Screen / Esc

Printer-friendly Version

Interactive Discussion

Principal components of particle size distributions

F. Costabile et al.

Title Page

Abstract

Introduction

Conclusions

References

Tables

Figures

⏪

⏩

◀

▶

Back

Close

Full Screen / Esc

Printer-friendly Version

Interactive Discussion



A first data set (*long-term experiment*) includes long-term ambient particle size distribution measurements at *three* observation sites in the Leipzig area. Particle size distributions (size range 3–800 nm) were recorded continuously during 2005 and 2006 at a rural, an urban background, and a street canyon site.

5 A second data set (*intensive spatial experiment*) comprises simultaneous size distribution measurements at a maximum of *eight* observation sites. Six out of the six fixed measurement sites were within a distance of 3 km in the downwind plume of Leipzig's city centre (Fig. 1). The sites included two roadside sites (i.e. sampling points downwind a major road), four urban background sites, one rural background site, and
10 an additional mobile site. The short-term spatial experiment lasted about two months between March and May 2005, and its data are introduced here for the first time.

Figure 1 shows the location of the measurement sites on simplified maps of Leipzig (population ca. 500 000) and its surroundings, with major urban geographical features indicated through lines and symbols. The main characteristics of the sites are summarised in Table 1a while Table 1b compiles measurement-specific information. The
15 numbering of the sites follows their alignment from west to east, which is the prevailing wind direction.

2.2 Measurement sites

Site S1 (urban background): the temporary measurement site S1 was located in
20 Leipzig's suburb "Schleussig", 4 km south-west of the city centre (Fig. 1, right box). To the west, the site borders a residential area with a dense pattern of four-storey residential buildings. A wooded area of 2 km depth separates the site from the city centre on its eastern side. The site can be considered representative of urban background conditions in south-western Leipzig.

25 *Site S2 (urban background)*: the temporary measurement site S2 ("Inselstrasse") was located in a residential area approximately 1 km east of Leipzig's city centre (Fig. 1, lower left box). Site S2 can be taken representative of urban background conditions in the area between the city centre's high-trafficked ring road and the B2 national road,

which crosses the eastern suburbs in a north-to-south direction.

Site S3 (roadside): the temporary observation site S3 (“Listplatz”) was located near the crossing of several major roads, including the four-lane B2 national road. About 50 000 vehicles pass by the site per day (Fig. 1, lower left box). S3 was therefore the site most influenced by road traffic among all observation sites used in our work. The sampling inlet was mounted on the third floor of an office building, facing a small park area eastward. Free atmospheric flow is warranted for the wind directions Southeast, East, North and Southwest, while for westerly winds, a vortex is expected to develop in the lee of the five-storey building block.

Site S4 (urban background): the temporary measurement site S4 (“Rabet”) was located in a park, about 1.5 km distant from Leipzig’s city centre (Fig. 1, lower left box). The site was singular in that an undisturbed advection was possible from almost all directions. The surroundings of the site were plain grassland, with only a few scattered trees. The nearest street was Eisenbahnstrasse street, about 200 m to the north, which is also the approximate distance to Site S5 (below). The measurements at the site S4 can be considered the best approximation of undisturbed urban background conditions in the eastern suburbs of Leipzig. The aerosol observations were supplemented by NO and NO₂ measurements as well as wind speed and direction measurements by a sonic anemometer, 6 m above the ground.

Site S5 (roadside, also long-term measurements): site S5 “Leipzig-Eisenbahnstrasse” is a permanent observation site in a street canyon about 2 km east of Leipzig’s city centre (Fig. 1, lower left box). Particles are sampled at a height of 6 m above street level on the northern border of a regular street canyon (Voigtländer et al., 2006). The canyon is traversed by a moderately trafficked arterial street carrying about 10 000 vehicles per working day. Vehicles are counted continuously by an automated video detection system. The aerosol measurements are supplemented by nitrogen oxide (NO and NO₂) measurements as well as wind speed and direction measurements by a sonic anemometer, 4 m above roof-top level.

Site S6 (urban background, also long-term measurements): the sampling site S6

Principal components of particle size distributions

F. Costabile et al.

Title Page

Abstract

Introduction

Conclusions

References

Tables

Figures

⏪

⏩

◀

▶

Back

Close

Full Screen / Esc

Printer-friendly Version

Interactive Discussion

“Leipzig-lfT” is situated on the roof of lfT’s institute building, at a distance of about 1.5 km east of site S5 (Fig. 1, right box). Aerosol particles are sampled at a height of 16 m above the ground. Highly-trafficked roads touch the area only at distances of at least 100 m. Leipzig-lfT can be regarded as a location with a spatially homogenised urban background aerosol (Wehner and Wiedensohler, 2003). The aerosol measurements are supplemented by measurements of nitrogen oxide (NO and NO₂), sulfur dioxide (SO₂) and temperature.

Site S7 (rural background, also long-term measurements): in this work the atmospheric research station Melpitz serves as a rural background site, i.e. a site where urban influence is far. The station is located 50 km northeast of Leipzig (Fig. 1, upper left box). Flat grass lands, agricultural pastures and woodlands dominate the surroundings of the site within several tens of kilometers. The ambient particle size distribution measurements correspond to those documented in Engler et al. (2007).

Sites S8a-d (additional locations): a mobile laboratory inside a van was deployed during the short-term spatial experiment to characterise further sites (S8a-d; cf. Fig. 1, lower left box). These included three roadside sites and an additional urban background site (Tab. 1b). These measurements lasted between one and three weeks per site. Due to the short duration of the data collected at the sites S8a-d they were not included in any statistical analysis and served only for the illustration of the case studies.

Official monitoring sites LfUG (Saxonian Office for the Environment and Geology): The body of particle size distribution data at the sites S1-8 was complemented by routine observations from four additional stations of LfUG (L1-4). The parameters measured there include PM₁₀ mass concentration, the mixing ratios of NO, NO₂, SO₂, O₃, and CO, BTX (benzene/toluene/xylene) and basic meteorological parameters. The particular sites used were L1 (“Leipzig-Mitte”, roadside), L2 (“Leipzig-West”, urban background), L3 (“Collm”), L4 (“Delitzsch”, all regional background), and are depicted in Fig. 1. This body of data served primarily to characterise the large-scale pollution situation in Leipzig.

Principal components of particle size distributions

F. Costabile et al.

Title Page

Abstract

Introduction

Conclusions

References

Tables

Figures

⏪

⏩

◀

▶

Back

Close

Full Screen / Esc

Printer-friendly Version

Interactive Discussion

2.3 Instrumental

Particle number size distributions (PNSD) were determined at multiple sites using particle mobility spectrometers. The designs used were a) the custom-built twin differential mobility particle sizer (TDMPMS) on the basis of Vienna-type differential mobility analyzers and using dry sheath air (Birmili et al., 1999), (b) the scanning mobility analyser (SMPS) – similar to (a) but using a closed-loop sheath circulation and operating in scanning mode, and (c) the commercial SMPS, model 8085 (TSI Inc., St. Paul, MN, USA). The deployment of the eight instruments is keyed after site in Tab. 1b. Andersen PM₁₀ sampling inlets were deployed at each site to remove coarse particles.

In order to achieve a maximum comparability of the size distribution measurements at different sites, frequent instrumental intercomparisons were conducted. As a matter of convenience, site S5 was selected as the central comparison site during the short-term spatial experiment in 2005. Before and after deployment of the mobility spectrometers at the sites S1–4, S6 and S8, the corresponding instruments were compared against the TDMPMS at site S5 for a period of at least three days using ambient aerosol. From these intercomparison experiments, particle losses (due to diffusion) in each instrument were quantified as a function of particle size, and taken into account in the final version of the measurement data. After the corrections, we expect the measurements at all sites to be comparable within $\pm 10\%$ with respect to total particle number concentration and volume.

3 Data analysis

The data-sets from both the long-term and the intensive spatial experiment were processed by Principal Component Analysis (PCA). PCA is a classical technique for dimensionality reduction, which has found plenty of environmental applications including atmospheric aerosol research (Chan and Mozurkewich, 2007; Huang et al., 1999). To avoid confusion we will use the term “STA” (statistical analysis) instead of “PCA”

Principal components of particle size distributions

F. Costabile et al.

Title Page

Abstract

Introduction

Conclusions

References

Tables

Figures

⏪

⏩

◀

▶

Back

Close

Full Screen / Esc

Printer-friendly Version

Interactive Discussion

hereafter when referring to a particular PCA analysis run rather than to the method in general.

Table 2 describes the five different analyses (STA) described in this paper. To make a wider use of the existing body of data, different analyses were conducted making varying compromises between the length of the data set analysed, and the number of observation sites included in one analysis. In a particular analysis STA i , i indicates the number of sites whose data were combined and co-analysed. STA1/STA3 and STA7 can be seen as extremes, since STA1/STA3 use two years of simultaneous data at three sites, and STA7 uses 17 days of simultaneous data at seven sites. The notable difference between STA1 and STA3 was that in STA1 a PCA was carried out for each site individually, while in STA3 the data from all sites were combined and co-analysed. In STA4, STA6 and STA7 the data from all i sites were generally co-analysed.

In practice, the particle size distribution data in $dN/d\log D_p$ were first log-normalised, and then standardised to a zero mean and unit standard deviation. The normalised values (simply N hereafter) were arranged in five matrices, N1, N3, N4, N6, N7. In analogy to STA i , the number indicates the number of measurement sites whose data were combined into a single analysis. In a matrix N_i , each of the p columns represents a standardised concentration value N , varying with site as well as particle diameter, and each row represents the combined 30-min average observations at all sites simultaneously.

Subsequently, the data matrices were transformed by PCA into a representation based on a new set of orthogonal variables, i.e. principal components (PCs). Detailed descriptions of the PCA method have been given in a number of textbooks (e.g., Gnanadesikan, 1977; Morrison, 1976; Mulaik, 1972). Briefly, the variable transformation is achieved by rotating the existing system of orthogonal coordinates $N_1 \dots N_p$ into a new system of orthogonal, uncorrelated variables (PCs) with their associated eigenvectors. The PCs were obtained by Varimax rotation, i.e. a fraction as large as possible of the total variance in the data set shall be attributed to a number of PCs as little as possible. A major asset of PCA is that large environmental data sets with many input

Principal components of particle size distributions

F. Costabile et al.

Title Page

Abstract

Introduction

Conclusions

References

Tables

Figures

⏪

⏩

◀

▶

Back

Close

Full Screen / Esc

Printer-friendly Version

Interactive Discussion

variables can often be reduced drastically to a simplified description using only a few PCs without the loss of relevant information.

Several criteria have been developed to identify the number of PCs (q) that should be retained as relevant for the description of the data set. In our work we used a combination of the Kaiser criterion (i.e. retention of PCs whose eigenvalue is greater than 0.65–1) (Pugatshova et al., 2007; Eder, 1989) as well as scree plot criteria (e.g., Chan and Mozurkewich, 2007) to determine the final number of PCs to retain. Also, the retained PCs $PC_1 \dots PC_k$ were arranged in decreasing order of their variance explained (λ_k), i.e. PC1 is the component exhibiting the largest single variance. λ_k is also called the eigenvalue of PC_k . Each eigenvector is composed of scalar coefficients, which describe the new PCs as a linear combination of the original variables $N_1 \dots N_p$. The coefficients thus represent the relative weight of each original variable in each PC. The so-called “factor loadings” represent the coefficients for PC_k scaled by the amount of variance λ_k explained by this PC (eigenvalue). They thus represent the relative weight of each variable in each PC re-scaled by the amount of variance explained by the PC.

Since the variables N had different scales, we decided to work with correlations instead of covariances. Hence, it was possible to directly link the loadings to the correlations among the original variables within each PC. Also, the eigenvectors with the largest eigenvalues corresponded to the dimensions with the strongest correlation in the data set.

Finally, the time scores of the new PCs – estimated by the loadings and the standardised values of N , were used as an input for a consecutive principal component analysis (STAc) including additional variables, i.e. pollutant concentrations, meteorological parameters and traffic volume. The goal of STAc was to relate the new PCs with these environmental variables and hence to provide some evidence on the atmospheric processes or particle sources associated with the new PCs. In STAc, the additional parameters were again log-scaled and standardised to zero mean and unit variance whilst the scores from STA1, STA3, STA4, STA6, and STA7 were not standardised again.

Principal components of particle size distributions

F. Costabile et al.

Title Page

Abstract

Introduction

Conclusions

References

Tables

Figures

⏪

⏩

◀

▶

Back

Close

Full Screen / Esc

Printer-friendly Version

Interactive Discussion

4 Results

4.1 Basic phenomenology

4.1.1 Mean particle number size distribution

To illustrate several basic features of our experimental data, mean size distributions as well as selected meteorological case studies are introduced. Figure 2 shows the mean size distributions of the two main data sets. The upper part of the figure presents 2 years of measurements at 3 sites (i.e. the long-term experiment) while the lower part shows the overall statistics of almost 2 months of measurements at 7 sites (i.e. the intensive spatial experiment).

It is very apparent that the mean particle number concentrations increase with decreasing distance to the main anthropogenic source, motor traffic. Below 300 nm particle diameter, the mean concentration at the traffic site is up to one order of magnitude higher than at the rural site Melpitz, which is located 50 km off Leipzig. Above 300 nm, however, the differences become minor, since these particles represent to a greater extent the long-lived regional aerosol.

The standard deviation of the data (i.e. the square root of the sample variance) is similar, but less obvious with respect to the proximity to the traffic sources. It is common to all sites that the highest variance in the data occurs in the UFP size range, particularly below 40 nm. Not unexpectedly, the traffic sites (S3 and S5) feature the highest variances, with wide local maxima in two modes between 10–20 and 50–100 nm, respectively. At both urban background and rural sites (S1, S2, S4, S6, and S7) the variance exhibits one local maximum around 20, and 70 nm, and another around 200 nm. The concentration variance is the lowest at the rural site with the exception of the size range below 20 nm.

Principal components of particle size distributions

F. Costabile et al.

Title Page

Abstract

Introduction

Conclusions

References

Tables

Figures



Back

Close

Full Screen / Esc

Printer-friendly Version

Interactive Discussion

4.1.2 Multiple-site case studies

High spatial homogeneity of aerosols under sunny conditions

Figure 3a illustrates the particle number size distributions measured during the intensive spatial experiment on 3 April 2005. Size distributions were measured at 6 sites in Leipzig concurrently. (Two sites included in the full set-up were not operational yet.) Since the day was a Sunday, the influence of traffic was low compared to weekdays. The levels of solar radiation indicate a cloudless day under relatively constant and slow south-easterly winds. The day started with PM₁₀ mass concentrations up to 40 μg m⁻³ in the rural background (sites L1 and L3), and up to 50 μg m⁻³ within the city (sites L2 and L4). SO₂ concentrations (not shown) were around 6 ppbV. After 10:00 h LT, PM₁₀ concentrations started to decrease significantly, most likely as a result of vertical dilution with cleaner air aloft. This decrease can also be clearly seen in all particle size distributions in the shape of a decrease of Aitken and accumulation mode particle number concentrations (Fig. 3a). The minimum in accumulation mode number concentration was reached at all sites simultaneously after 15:00 h.

In the contour diagrams, it can be seen that new secondary particles – suggested to originate from photochemical processes, were formed at all sites. The “banana”-shaped events were characterised by an increase in particle number concentrations below 10 nm around 10:00 h. It can be seen very clearly that this increase happened simultaneously at all sites, including the rural site Melpitz (S7), which is at a distance of 50 km from Leipzig. The smooth evolution of the size distributions (particle formation and subsequent growth) on 3 April 2005 at all sites suggests a very high spatial homogeneity of the aerosol across the entire city and its surroundings. This homogeneity can be observed despite the sites not being aligned on this day with respect to the prevailing southerly wind direction (cf. Fig. 1). The case of 3 April 2005 demonstrates that under sunny conditions and the reduced impact of traffic emissions (Sunday) the particle size distribution can be distributed very homogeneously in space over at least 50 km, even including urban zones.

Principal components of particle size distributions

F. Costabile et al.

Title Page

Abstract

Introduction

Conclusions

References

Tables

Figures

⏪

⏩

◀

▶

Back

Close

Full Screen / Esc

Printer-friendly Version

Interactive Discussion

Principal components of particle size distributions

F. Costabile et al.

[Title Page](#)[Abstract](#)[Introduction](#)[Conclusions](#)[References](#)[Tables](#)[Figures](#)[⏪](#)[⏩](#)[◀](#)[▶](#)[Back](#)[Close](#)[Full Screen / Esc](#)[Printer-friendly Version](#)[Interactive Discussion](#)*High spatial homogeneity of aerosols under cloudy conditions*

Figure 3b illustrates, like the previous example, a case of high spatial homogeneity of the particle number size distribution as well as PM_{10} concentration across the entire Leipzig area. (From here, particle size distribution measurements were operational at 8 sites simultaneously.) In contrast to Fig. 3a, this day (24 April 2005) was cloudy, with north-east being the prevailing wind direction. Generally, relatively smooth changes can be seen throughout the day in the particle number size distribution; between midnight and the afternoon (14:00 h), a nearly constant Aitken mode dominates the size distribution. Its mode diameter slowly shifts from 40 nm to about 70 nm during the morning. Between 14:00 and 17:00 h, an event of secondary particle formation (<20 nm) can be seen, which is evidenced by the slow growth of its nucleation mode (Fig. 3b). Its peak concentrations were, however, much lower than on the case shown in Fig. 3a. This second week-end case demonstrates that the particle size distribution can be homogeneously distributed in space under various wind directions and in the presence of clouds as well.

A week-day with secondary new particle formation

Figure 3c illustrates the dynamics of the particle number distributions on a week-day, 20 April 2005. Like in Fig. 3b, the wind direction was north-easterly, but the wind speed was considerably higher and intensive solar radiation prevailed. PM_{10} mass concentrations were very similar across the entire region ($25 \mu\text{g m}^{-3}$) except at the city centre site L2 (up to $100 \mu\text{g m}^{-3}$), which suffered from exceptional local contamination by construction activities at the time. In Fig. 3c, a clear impact of traffic emissions can be seen in the morning between 06:00 and 10:00 h at the traffic site S5. It can be recognised as a size distribution peak around 20 nm. (It is worth mentioning that the street canyon at site S5 is oriented in east-west direction, and that the northerly winds place the sampling inlet there in the leeward position of the traffic – this is the supposed reason for the high concentrations here.)

A “banana”-shaped event of new particle formation and growth starts around 12:00 h

Principal components of particle size distributions

F. Costabile et al.

[Title Page](#)[Abstract](#)[Introduction](#)[Conclusions](#)[References](#)[Tables](#)[Figures](#)[⏪](#)[⏩](#)[◀](#)[▶](#)[Back](#)[Close](#)[Full Screen / Esc](#)[Printer-friendly Version](#)[Interactive Discussion](#)

across the entire city. The start time can be determined with confidence at those sites with 3 nm as a lower cut-off diameter of the measurement (S1, S5, S6, and S7); at the sites with 10 nm cut-off, the event can only be detected with a noticeable delay. The rural site makes an exception in that the formation event starts earlier, before 10:00 h, which indicates a certain spatial inhomogeneity of the formation event. It is worth mentioning that around 14:00 h the particle mode originating from the traffic emissions in the morning disappears almost completely, and at all the urban sites (Fig. 3c). This disappearance is again interpreted as the impact of vertical mixing rather than the decrease of traffic emissions because real-time traffic counts suggest a nearly unchanged traffic volume until 18:00 h. The case of 20 April 2005 demonstrates urban and regional spatial homogeneity of the aerosol again, however, with limitations at the traffic sites and the distant rural site.

A week-day with limited pollution impact

Figure 3d illustrates a week-day case under slow westerly winds. In contrast to the previous cases, PM_{10} concentrations are quite inhomogeneous across the entire region. Low background aerosol concentrations can be seen best in PM_{10} at site L3, and in low accumulation mode concentrations at the sites S7 (rural), S1 and S4 (both urban background). The influence of motor traffic manifests itself throughout most of the day, starting just before 05:00 h, and highly evident at S3, S5, and S8a, which are all roadside observation sites. The impact of traffic can also be seen in high levels of NO_x (not shown). The highest traffic-induced concentrations occurred at site S5. Fluctuations in the traffic signal can be best seen at the temporary site S8a, which had measurements at a high time resolution of 6 min. Individual peak concentrations could also be detected at site S2, which was therefore considered as the urban background site influenced most directly by traffic sources.

The pattern of fluctuating signals caused by traffic sources are overlaid by a secondary particle formation event starting at 13:00 across the entire city (S1–S6, and S8a). This occurred under sunny conditions when the horizontal wind speed (not

shown) reached a minimum. Like the previous cases, and as in many examples in the literature, vertical mixing was a factor associated with the formation event. As can be seen especially for site S5 in Fig. 3d, the signal of the secondary particles overlays with the traffic-derived particles after 16:00 h. Both cannot be distinguished any more.

5 At the rural site S7, the particle formation event appears not to be the same as in the city, with lower concentrations and a significant time delay, which indicates spatial inhomogeneity. In summary, Fig. 3d demonstrates a very inhomogeneous spatial distribution of nearly all aerosol components, with the single exception of a secondary particle formation event that occurred across the entire city.

10 A week-day with high pollution impact

Figure 3e illustrates another case – 12 April 2005, when the impact of local sources can be clearly seen across the entire city of Leipzig. Several features were similar to Fig. 3d, such as the slow winds, the great regional inhomogeneity of PM₁₀. However, 15 the solar radiation was even lower, thereby providing less convective forcing to facilitate vertical atmospheric mixing. As a consequence, the impact of local sources, most of all traffic, can be seen throughout almost the entire 24 h. Very high particle concentrations (more than 50 000 cm⁻³ in $dN/d\log D_p$) could be seen over several hours at the traffic sites S3, S5, and S8a, while this value was reached briefly at the 20 background sites S2 and S6 as well. In summary, this day demonstrates the possibility of high anthropogenic aerosol concentrations at many sites across the entire city of Leipzig. Poor mixing prevailed, which is also symptomatic in the way that no secondary particle formation could be observed on this day.

25 A week-day featuring several aerosol types

Figure 3f shows a last case study, featuring the succession of several aerosol types across the city during relatively warm weather on 15 April 2005 (up to 27°C). The impact of traffic emissions in the morning can be seen at all sites, sharply delimited between 06:00 and 12:00 h. On this morning, the highest particle number concentra-

Principal components of particle size distributions

F. Costabile et al.

Title Page

Abstract

Introduction

Conclusions

References

Tables

Figures

⏪

⏩

◀

▶

Back

Close

Full Screen / Esc

Printer-friendly Version

Interactive Discussion

tions occurred at site S3, which illustrates that the ultimate amplitudes of the signals at the traffic sites S3 and S5 are not scalable with each other but likely depend on the micrometeorological factors (wind) in their immediate surroundings. Between 02:00 and 05:00, a local plume of particles centered around 30 nm could be detected exclusively at the neighbouring sites S2 and S3. This example shows that multiple-site measurements are needed if such local plumes of a scale of a few 10 or 100 m should be resolved.

In the afternoon, a double-peaked plume could be detected across the entire city between 15:00 and 19:00. It shows two subsequent and distinguished modes centered around 20 and 30 nm, respectively. It is intriguing that such a plume of relatively moderate concentration (compared, e.g., to the particle formation events shown above) can be detected across the entire city. The most persistent aerosol mode, both in time and space, was an accumulation mode centered around 150 nm. It prevailed after 08:00 h, and could be seen in almost pure shape at the sites S1, S2, S3, S4, and the low-trafficked roadside site S8b, while it was masked by local emissions especially at site S5. This last case study reveals some unexpected spatial correlations of aerosol components across the entire city, but also several small-scale phenomena which could be seen at a maximum of two sites.

In general, the discussion of the case studies reveals a wide spectrum of size-segregated aerosol components that occur across the entire urban atmosphere under study. In order to capture the wealth of information contained in such an atmosphere, spatially resolved measurements are clearly advisable. Meanwhile, clear correlations between different observation sites were found for particle populations across the entire sub- μm particle size spectrum. Such correlations concerned the biggest particles in the accumulation mode (also seen in total particle mass), but also the smallest detectable particles in the nucleation mode. To establish the relative relevance of the many phenomena described, the data sets need to be analysed statistically; this is provided in detail in the following.

Principal components of particle size distributions

F. Costabile et al.

Title Page

Abstract

Introduction

Conclusions

References

Tables

Figures



Back

Close

Full Screen / Esc

Printer-friendly Version

Interactive Discussion



4.2 Multiple-site principal components in the particle size distribution

In the previous Section we showed the existence of large-scale components (i.e. such being representative for a larger spatial scale) of the PNSD. Here, the results of the principal component analysis (PCA) at single (STA1) and multiple sites (STA3, STA4, STA6, and STA7) are presented, which characterise co-variations in the PNSD both in space and time.

4.2.1 Single-site principal component analysis

Figure 4 shows the results of principal component analyses carried out for the long-term particle size distribution data at each of the three sites S5, S6, and S7 separately. These analyses correspond to STA1, described in Table 2. Importantly, STA1 is able to extract all the modes identified above in terms of local maxima in the size distribution of the particle number variance. 6 very similar principal components (PCs) could be extracted from each data set. The loadings of PC2 peak in the nucleation mode (5–25 nm), of PC3 in the Aitken mode (20–60 nm at the urban background and rural sites, and 20–100 nm at the roadside), and of PC5 in the accumulation mode (70–300 nm). Additional components with loadings peaking in the accumulation and nucleation mode range were found, which will be discussed later. The basic outcome is that the single-site STA was able to reproduce the major features of the temporal variability of the PNSD. With the single-site STA, however, no information can be retrieved on possible covariations of the PNSD in space.

4.2.2 Components in the spatial data set

In addition to several “noise” PCs – explaining the lower part of the variance – STA7 (Fig. 5a) reveals three “signal” PCs – features always present – and four “mixed” PCs – features present in part of the dataset. The first signal PC represents large-scale PNSDs with a distinct accumulation mode (>200 nm), and likely refers to regional

Principal components of particle size distributions

F. Costabile et al.

Title Page

Abstract

Introduction

Conclusions

References

Tables

Figures

⏪

⏩

◀

▶

Back

Close

Full Screen / Esc

Printer-friendly Version

Interactive Discussion

aerosols. The second and third signal PCs represent PNSDs with aged nucleation (PC2) and Aitken modes (PC3) – their very high spatial correlations suggest new particle formation and growth events. Two similar mixed PCs (PC4 and PC5) show then a very wide Aitken mode characteristic of the two traffic sites - they probably hence represent urban traffic.

Notably, no significant difference is found when the rural site is not included in the STA (Fig. 5b). The three signal PCs and the two mixed PCs before mentioned are still the same indeed, and changes are only found in the noise PCs. This result implies the spatial scale of the before mentioned signal and mixed PCs to be as big as the all study area.

On the other hand, STA4 (Fig. 5c) showed, in general, similar signal and mixed PCs related to the accumulation, Aitken, and nucleation modes. However, the wider size range of the measurements (cf. Table 2) produced apparently much more complex results – two further PCs in the Aitken and accumulation mode size range, and an even more complex nucleation mode. This fact is better discussed in the following paragraph.

4.2.3 Components in the long-term data set

STA3 (cf. Table 2) reveals three “signal” PCs (Fig. 5d) with modes in the size range (cf. Table 3) of 300–800 nm (PC1), 90-250 nm (PC3), 4-20 nm (PC2 - we will call it “traffic” type since it loads highly at the roadside). An additional signal component (PC8, 30–200 nm) is found, quite similar to the before mentioned PC4 and PC5 of STA7. Further “mixed” PCs in the nucleation mode range have higher loadings at the rural (PC4, 5–20 nm) and the urban background sites (PC6, 3–15 nm).

To put these findings into perspective, we compared the results of the various STAs: In STA1, the nucleation mode PC2 is a signal PC at all of the sites (Fig. 4); however, only at the roadside PC2 of STA1 exhibits also a correlation with bigger particles up to 100 nm. This correlation manifest itself by the right tail of the loadings curve of PC2 of STA1, and is similarly found in PC2 of STA3 (Fig. 5d). Moreover, a PC4 with

Principal components of particle size distributions

F. Costabile et al.

Title Page

Abstract

Introduction

Conclusions

References

Tables

Figures



Back

Close

Full Screen / Esc

Printer-friendly Version

Interactive Discussion



mode diameter <5 nm appears in all the STA1; however, because of its low variance no related PC is extracted by the multi-site STA3. Remarkably, the PC4 with the highest variance is extracted by STA1 at the urban background site. As well, PC6 of STA3 (Fig. 5d), which mainly loads at the urban background site (we will call it “urban” type), has the lowest mode diameter. We will discuss this point later as indications of either different nucleation processes or nucleation processes with low correlations in space.

In the Aitken mode range, STA3 extracts three mixed PCs (PC5, PC13 and PC7, Fig. 5d). Both PC5 and PC13 have higher loadings at the urban background sites (“urban Aitken”), but the mode of PC13 is shifted towards larger values (30–90 nm) – same as the signal PC3 of STA4, STA6, and STA7 (Fig. 5a). PC7 of STA3 has instead higher loadings at the rural site (“rural Aitken”) with a smaller mode diameter (20–70 nm) – as PC8 of STA4 and PC14 of STA7.

In the accumulation mode, the two signal PC1 and PC3 of STA3 (Fig. 5d) are probably connected with the “droplet mode” (John et al., 1990; Meng and Seinfeld, 1994) and the “condensation mode” (Seinfeld and Pandis, 2006). Contrary to PC1, which has the highest spatial correlation, the spatial scale of PC3 depends on the distance from traffic sources. The larger the distance, the higher the loadings. Interestingly, the Aitken and accumulation mode PC1, PC3 and PC5 of STA1 (Fig. 4) are clearly separated only at the non-traffic sites. (Note that PC5 is not a signal PC at the site No. 5). It is probably PC8 of STA3 (Fig. 5d) which explains this difference. PC8 correlates not only 30–200 nm particles at the traffic sites, but also 80–100 nm particles at the urban and rural background sites. Hence, PC8 seems to be an urban-scale component (we will call it “urban traffic”), rather than local traffic emissions. (Local traffic emissions are better represented by the PC3 of the roadside STA1, Fig. 4).

Principal components of particle size distributions

F. Costabile et al.

Title Page

Abstract

Introduction

Conclusions

References

Tables

Figures

⏪

⏩

◀

▶

Back

Close

Full Screen / Esc

Printer-friendly Version

Interactive Discussion

4.3 Dependencies of size distribution components: diurnal behavior and correlations

4.3.1 Temporal cycles

A general observation was that the presence of high scores was limited to a couple of hours for all nucleation PCs, in the order of several hours for the Aitken, and to days for the accumulation mode PCs. Weekly cycles may be seen for the all PCs with modes below 30 nm (PC2, PC4, PC6, PC5) and for the “urban traffic” PC8 (Fig. 6). This suggests common traffic source dependence.

All UFP-related PCs, including the “condensation mode” PC3, have both diurnal and seasonal cycles (Table 3). The scores are always higher in summer but for the droplet mode, the long-range transport, and the urban traffic PC8; nucleation (PC2, PC4, PC6) and condensation (PC3) mode PCs have generally higher scores at day-time, and Aitken mode PCs (PC5, PC7, PC13) in the late evening/early morning or the night-time. This probably reveals the relative importance of photochemically induced factors.

4.3.2 Inter-correlation

The consecutive STAc (cf. Sect. 3) calculated for all STAs gave similar results in terms of inter-correlations with meteorological and air pollution variables, as well as intra-correlation between PC scores (see Sect. 4.3.3). Table 3 lists these correlations.

Meteorological variations alone showed very weak correlations with the extracted PCs. However, remarkable inter correlations were found in connection with air pollutants.

Notably, of all the investigated parameters only PM₁₀ has no more than one significant correlation. It is with the accumulation mode PC1 of STA7 (Fig. 5a), and with SO₂ and benzene concentrations, suggesting this PC1 to represent long-range transport particles. This finding indicates extremely different behaviours of PM₁₀ and UFPs.

Oppositely, the relative humidity seems to correlate with all the retained PCs. The

Principal components of particle size distributions

F. Costabile et al.

Title Page

Abstract

Introduction

Conclusions

References

Tables

Figures

⏪

⏩

◀

▶

Back

Close

Full Screen / Esc

Printer-friendly Version

Interactive Discussion

correlation with the droplet mode PC is always positive and quite considerable. The anti-correlations with the UFP-related PCs are, instead, perhaps connected with global radiation, temperature, and ozone. At daytime, for higher light-duty vehicle flows, an interesting time correlation at the background sites was revealed between nucleation mode PCs (inverse correlation), Aitken and condensation mode PCs (direct correlation), ozone (direct correlation), and benzene and NO_x (inverse correlation) (cf. Table 3).

The results also indicate time correlation between the measured SO₂ concentrations and the nucleation mode PCs at the urban background sites (cf. Table 3). Perhaps it should be noted as this correlation was probably masked by the fact that higher SO₂ concentrations at daytime occurred during two different situations of high pressure: long-range transport due to winds from E/NE, and urban plumes with south-westerly winds. Only the second case was not correlated with bigger particles. For the first case, a higher condensation sink can be expected, and thus a much lower or no nucleation at all.

It should be noted that UFPs were always inter-correlated at the traffic sites. In STA3 (Fig. 5d), in addition to the high correlation with PC8, traffic flows correlate directly with the traffic- and urban-type nucleation PC2 and PC6, and the condensation mode PC3 during the rush hours, and inversely with the urban Aitken mode PC13 and rural type nucleation PC4. The correlation with the traffic-type nucleation PC2 is somehow interesting. In STA1 (Fig. 4) it is the PC4 (mode <5 nm) that only correlates with traffic flows and (upwards) vertical wind speeds – PC2 also correlates with other meteorological parameter. PC2 increases together with traffic flows, but with rates of increase anti-correlated with it – the correlation being direct with LDV, and inverse with HDV at daytime. This point will be later discussed as a possible evidence that only PC4 (mode <5 nm) of STA1 represents traffic emitted particles.

Principal components of particle size distributions

F. Costabile et al.

Title Page

Abstract

Introduction

Conclusions

References

Tables

Figures

⏪

⏩

◀

▶

Back

Close

Full Screen / Esc

Printer-friendly Version

Interactive Discussion

4.3.3 Intra-correlation

The above introduced inter-correlations were always quite weak, and surely weaker than the intra-correlations among the PC scores themselves (according to STAc, cf. Table 3). These time correlations were always notably higher than 0.5.

As a general finding, the highest scores of fresh, aged nucleation and Aitken mode PCs followed each other in time, and were all strongly anti-correlated with the scores of the larger particles. Interestingly, these relations were more clear during large-scale events of new particle formation and growth (for lower scores of the accumulation mode and urban traffic PCs). Perhaps it is worth noting that the “urban traffic” PCs (e.g. PC8 in STA3) correlated with the other PCs in a way similar to what previously discussed for traffic flows.

4.4 Signature size distributions

“Signature size distributions” were calculated on the basis of the PCA coefficients, and are displayed in Fig. 7. Three analyses, STA7, STA4 and STA3 are covered.

During the intensive spatial experiment in spring time 2005 – analysed by STA7, the signature PNSDs at urban background sites are dominated by long-range transport (PC1 in Fig. 7a) and new particle formation and subsequent growth events (PC2 and PC3 in Fig. 7a). Particles in the nucleation mode range at the traffic sites S3 and S5 are naturally influenced by direct local emissions as well (PC4 and PC5 in Fig. 7a).

It is interesting that the nucleation mode component PC2 in Fig. 7a shows a very similar size-dependent profile across all sites, whether urban background or roadside. It has therefore been a conclusion that PC2 represents a size distribution component that is spatially homogeneous. We assume that this particle component with a concentration maximum just below 20 nm has its origin, in part, from direct traffic emissions present over the whole city, which are mixed downwind the sources into the urban roughness layer and, secondly, from gas-phase nucleation and subsequent growth processes across the whole city as well. Within STA7 it was not possible to distinguish

Principal components of particle size distributions

F. Costabile et al.

Title Page

Abstract

Introduction

Conclusions

References

Tables

Figures



Back

Close

Full Screen / Esc

Printer-friendly Version

Interactive Discussion

these two likely processes due to the limited size range of the data, starting only at 10 nm diameter, and maybe to the limited duration of this particular data set. It seems that particles originating from both processes overlap in the size spectrum of that component and, owing to the mixing processes in the urban boundary layer, these processes cannot be distinguished any more at true urban background site, i.e. sufficiently downwind of the traffic sources themselves.

At the rural site, new particle formation and related particle aging (PC6 and PC14 of STA7) have a more important effect than in the urban area. A condensation mode (PC3 of STA4, cf. Fig. 5c) is clearly an other important factor particularly at the background sites (Fig. 7b), where its effect is probably not masked by the local traffic emissions. Significant variations are still produced in the droplet mode (PC1 of STA4).

When considering the long-term experiment (Fig. 7c), the new particle formation at the rural site (PC4 of STA3, Fig. 5d), and the accumulation mode particles (both droplet and condensation mode PC1 and PC3 of STA3) still dominate the PNSD. However, “urban traffic” (PC8 of STA3) appears to be more relevant than during the spring campaign, and produces noteworthy variations even at the rural site. Aged nucleation mode particles considerably affect the PNSDs at both the urban and rural background sites (PC5 and PC7 of STA3), whilst fresh nucleation mode particles reveal very peculiar signatures, which will be discussed in the following section.

5 Discussion

5.1 A critical look at PCA: what can it provide? What does it mean?

Given sufficient data, PCA is theoretically the optimal linear scheme, in terms of least mean square error, for compressing a set of high dimensional vectors into a set of lower dimensional vectors, and finally reconstructing the original set (e.g., Gnanadesikan, 1977; Morrison, 1976; Mulaik, 1972). However, the results provided by PCA are limited by the assumptions made in its derivation, which are the linearity of original variables,

Principal components of particle size distributions

F. Costabile et al.

Title Page

Abstract

Introduction

Conclusions

References

Tables

Figures

⏪

⏩

◀

▶

Back

Close

Full Screen / Esc

Printer-friendly Version

Interactive Discussion

the orthogonality of principal components, the statistical importance of mean, standard deviation and correlation, as well as the assumption that large variances have relevant dynamics. These assumptions require probably particular consideration.

On one hand, the last assumption would imply that only if the observed data have a high signal-to-noise ratio, the larger variance PCs correspond to interesting dynamics and the lower ones to noise. By making use of both the Kaiser and scree plot criteria, we retained only PCs representing critical features in the dataset – the higher variance or “signal” PCs, and events that happened in a relevant portion of the data set, the “mixed” PCs. This means that rare and/or local features are not included in the scope of our analysis. In fact, “noise” PCs should not explain long-term and large-scale tendencies of PNSD variability.

On the other hand, each PC extracted by the multi-site PCA represents an independent statistical deviation of PNSD from its average value in both space and time. This deviation was found to be uniquely characterised by one higher statistical variance of one particular size range (i.e., the mode). This was probably also influenced by the calculation of loadings in terms of correlations. Hence, each PC-discriminating factor is probably linked to a common process, which correlates in both space and time distinctive PNSD “states”. In the single-site STA1, the word “state” can probably be explained in terms of the PNSD temporal variability (cf. Fig. 2 and Sect. 4.1). This approach would agree with earlier uses of a “measurement variability” to understand timescales of PNSD (Junge, 1974; Jobson et al., 1998), where the “states” could identify “typical” size distributions (Tunved et al., 2004), or sources (Chan and Mozurkewich, 2007). However, in this work, the multi-site PCA contemporary considers both the spatial and the temporal correlations. In this sense, even if the different PCs are not truly Lagrangian in that one always follows the other in time, the analysis of the states represented by these PCs might likely help to understand how the different aerosol aging processes are related to each other in a Lagrangian perspective. With this in mind, a deeper discussion of the results is provided in the followings.

Principal components of particle size distributions

F. Costabile et al.

Title Page

Abstract

Introduction

Conclusions

References

Tables

Figures



Back

Close

Full Screen / Esc

Printer-friendly Version

Interactive Discussion



5.2 Spatio-temporal variability of the size distribution

The spatio-temporal variability of PNSD in the urban and suburban atmosphere of Leipzig was found to be a complex phenomenon. The mean size distributions at different sites were observed to vary greatly notably with respect to the proximity of traffic sources. When examining the Pearson rank correlation coefficients between different sites we found the highest correlations (0.85–0.95) for diameters above 100 nm, in the accumulation mode, between urban background sites, and the lowest ones (0.2–0.3) below 20 nm, in the nucleation mode, between rural and traffic sites. This finding is in obvious agreement with previous experimental studies covering the same subject (Wehner et al., 2002; Ketzel et al., 2004; Hussein et al., 2005; Tuch et al., 2006; Pustinen et al., 2007; Mejia et al., 2008).

However, we could identify several large-scale factors in the aerosol size distribution. Importantly, these independent statistical factors seem to be present not only in the accumulation mode, but also in the UFP size range. In the following we discuss the behaviour of these factors in time and space in more detail, and draw connections to the established particle modes.

5.2.1 Statistical factors in the accumulation mode range

The statistical factor covering the highest variance in the overall data set resides in the accumulation mode (PC1 in each of STA7, STA4 and STA3). Meanwhile this factor represents the one with the lowest spatial variation observed in our experiment. Low temporal and high spatial homogeneity also imply a long life-time of these particles. These features are also a consequence of the accumulation mode being the least affected by aerosol dynamical processes, including coagulation and sedimentation (Hinds, 1999; Seinfeld and Pandis, 2006). Wet deposition seems essentially to be the limiting factor for the life-time of continental accumulation mode aerosol (Andronache, 2004).

An interesting because slightly unexpected result is the obvious separation of the variance of the accumulation mode into two distinct factors (PC1 and PC3 in STA3;

Principal components of particle size distributions

F. Costabile et al.

Title Page

Abstract

Introduction

Conclusions

References

Tables

Figures

⏪

⏩

◀

▶

Back

Close

Full Screen / Esc

Printer-friendly Version

Interactive Discussion

cf. Fig. 5). We speculate that these two factors correspond to two aerosol particle populations identified before, the “condensation mode” (Seinfeld and Pandis, 2006), i.e. accumulation mode particles containing aged secondary aerosol and also direct anthropogenic emissions, and the “droplet mode” (John et al., 1990; Meng and Seinfeld, 1994), i.e. particles that underwent fog or cloud activation and increased their size by liquid phase chemical reactions.

Notably, the spatial and temporal variability of the droplet mode (centered around 400 nm) is lower than that of the condensation mode (centered around 150 nm). In fact, the droplet accumulation mode is the aerosol factor that is most homogeneous in space and time. As the droplet mode was positively correlated with relative humidity (cf. Table 3), we interpret this mode being controlled by the large-scale synoptic weather. Humid air masses that have the potential for cloud activation are apparently required to produce this mode (Hering and Friedlander, 1982).

In contrast to the droplet mode, the condensation mode state was shown to have the higher factor loadings the farther the site was from traffic sources. Positive correlations occurred with temperature, global radiation, and ozone, but not with NO_x (cf. Table 3). Consistent with the observations of McFiggans et al. (2005), it also correlated with gas phase CO and benzene, which are good markers for traffic-related emissions. Mass spectrometric analyzes have frequently identified a mass mode composed mainly of organic material at diameters of about 100–200 nm at observation sites affected by fresh pollution or urban air masses (McFiggans et al., 2005; Drewnick et al., 2004; Jimenez et al., 2003). We speculate that these observations correspond to the aerosol mode identified as the “condensation mode” in our analysis. An immediate consequence is that the condensation mode part of the accumulation mode cannot be regarded as a purely long-range transported aerosol but is influenced by primary particle emissions and secondary aerosol formation within the urban and suburban atmosphere.

Principal components of particle size distributions

F. Costabile et al.

Title Page

Abstract

Introduction

Conclusions

References

Tables

Figures



Back

Close

Full Screen / Esc

Printer-friendly Version

Interactive Discussion

5.2.2 Statistical factors in the Aitken mode range

Aitken mode particles (around 30–90 nm) were represented by more than one PC, more specifically such representing urban (PC3 in Fig. 5c, and PC5 and PC13 in Fig. 5d) and rural observations (PC8 in Fig. 5c, and PC7 in Fig. 5d).

The urban types scores were higher during the early morning, while the rural types scores higher in the late evening (cf. Fig. 6). Though different, some time correlations were found between these components that obviously belonged to similar sources or processes (cf. Sect. 4.3.3.). In the rural area, less affected by traffic emissions, smaller Aitken particles (PC7 of STA3) could have been grown mainly due to coagulation and/or condensation processes from locally nucleated particles (PC4 of STA3). Contrarily, in the urban area Aitken particles (PC13 of STA3) could have also started their atmospheric life as primary traffic particles (PC5 of STA3), growing then by coagulation and/or condensation (during periods of lower emissions, as suggested by the lower scores at daytime).

The analysis hence reveals the urban Aitken mode particles to have a spatial scale as large as the city, to result from the complex interaction of both primary and secondary sources, and to be more persistent and have larger diameters in the urban than in the rural area.

5.2.3 Statistical factors in the nucleation mode range

Our size distributions of the nucleation mode could be broken down into three size intervals corresponding to different behaviors: <5 nm, 3–20 nm, and >10 nm (cf. Table 3). The highest spatio-temporal correlation occurred in the size interval >10 nm (cf. PC2 of STA7, Fig. 5a). However, the identification of this nucleation mode component was not the same during all individual PCAs: in STA4, which encompasses less sites than STA7 but a longer time period and wider size range as well as in STA3, which covers two years, this component is less evident because it is split among components characterizing single sites only. Another perturbation can naturally be the constraint of

Principal components of particle size distributions

F. Costabile et al.

Title Page

Abstract

Introduction

Conclusions

References

Tables

Figures

⏪

⏩

◀

▶

Back

Close

Full Screen / Esc

Printer-friendly Version

Interactive Discussion

10 nm as the lower cut-off size in STA7 compared to 3 nm in STA4. It is possible that the dominating role of PC2 in STA7 was caused by the high frequency of regional new particle formation events during the measurement period covered here. Similar results were found by a previous study, in the same region, during sunny conditions (Wehner et al., 2007).

The analysis of the long term data set provided statistically more robust results. The three components governing the 3–20 nm size range (PC2, PC4, PC6 in STA3; cf. Fig. 5d) represent particle formation processes characteristic of each of the three sites. We attribute this split-up mainly to different levels of exposure at the three sites, representing roadside, urban background, and rural conditions – but in the case of the rural site also to the spatial distance (50 km).

To better differentiate the nucleation mode components, average diurnal cycles of their scores are indicated in Fig. 8. On week-ends, the three components show very similar diurnal cycles peaking around mid-day. This is an argument for the components describing mainly the photochemically induced particle formation. (It has to be noted that the traffic emissions reach a maximum during mid-day on week-ends as well.) During weekdays, in contrast, the cycles show a multiple-peaked shape, most evident in PC2: a first peak (06:00–08:00) coincides with high traffic volumes in the rush hour. A second peak occurs after mid-day, which coincides with the cycle seen on the weekend. This mid-day peak is therefore associated again with secondary particle formation. In the case of PC8, i.e. the component most strongly related to traffic volume, a third peak can be seen around 16:00–18:00. This is interpreted as the evening rush hour.

Interestingly, PC2 exhibits a high temporal variability (see Fig. 2) and a clear correlation with larger particles (up to 100 nm), which point out to vehicle exhausts like for PC8. However, we believe that PC4 (mode <5 nm) of STA1 at the roadside (cf. Fig. 4a and Table 3) better represents engine related nucleation mode particles (Kittelson, 1998). It is “localised” (i.e., noise PC), and only correlates with traffic flows and vertical wind speed. In the case of PC2 there are both a much larger dependency on meteorology, and a much larger spatial correlation – up to 0.7 in the urban area and still

Principal components of particle size distributions

F. Costabile et al.

Title Page

Abstract

Introduction

Conclusions

References

Tables

Figures

⏪

⏩

◀

▶

Back

Close

Full Screen / Esc

Printer-friendly Version

Interactive Discussion

>0.3 with the rural site. We attribute this “signal” PC2 to urban traffic emissions which have already undergone processing on the time-scale of several tens of minutes. Also Chan and Mozurkewich (2007) found, at a single site only, similar results. As well, the existence in urban and suburban environments influenced by traffic emissions of an additional nuclei mode has been emphasized in previous works (e.g., Sioutas et al., 2005).

The “rural” type PC4 (Fig. 5d) has the lowest correlations both in space (0.2–0.4) and in time. This can be possibly explained by the twofold argument that the rural site is the farthest one from the urban area, and that the spatial scale of PC4 is likely lower than the distance from the urban sites. Notably, its signature (cf. Fig. 7b and Fig. 7c) indicates nucleating sources comparably much larger over rural than over the urban environment. One finding which is probably surprising are the higher scores during the week days. Traffic emissions seem to have enhanced the nucleation mechanisms even in the rural area.

The urban-type PC6 (see Fig. 5d) has the highest time correlation and an intermediate spatial variability (0.4–0.7). This is probably due to its smaller distance from the closer urban sites. It has higher scores at midday like the rural type PC4, but it is still modulated by the typical structure of the urban traffic PC8 (Fig. 8). Like the rural type PC4, it is higher during large-scale new particle formation and growth events (e.g., Fig. 3a), and is directly time correlated with temperature and global radiation, as well as with Aitken mode PCs. Like the traffic type PC2, it is enhanced by higher concentrations of gaseous pollutants (cf. Table 3). The highest scores occur for the observation site downwind of the city. More interestingly, this is the only urban-scale and long-term nucleation mode PC with a mode peak diameter below 8 nm (see Fig. 5d), and the only one with a significant correlation with SO₂ at daytime. Previous works pointed out to photochemical production in either urban (Kerminen and Wexler, 1996) or industrial plumes (Brock et al., 2002) containing SO₂. In fact, SO₂ oxidation products such as H₂SO₄ have long been considered precursors for newly formed particles (Doyle, 1961). It is probable that in the case of the rural type PC4, this correlation is masked by the

Principal components of particle size distributions

F. Costabile et al.

Title Page

Abstract

Introduction

Conclusions

References

Tables

Figures

⏪

⏩

◀

▶

Back

Close

Full Screen / Esc

Printer-friendly Version

Interactive Discussion

fact that SO₂ was measured only far from the rural site. Previous studies in rural atmospheres in Germany suggested mixed statistical effects of both, SO₂ mixing ratios as well as solar radiation for the onset of photochemically-induced particle formation (Birmili and Wiedensohler, 2000; Birmili et al., 2003).

In summary, the nucleation mode in the urban area tends to be more variable in time and space the smaller the particle diameters are. Particles below 5 nm appear to vary according to spatio-temporal scales smaller than the ones considered in this study. The growth of these smaller particles (<5 nm) to a larger sizes (8–10 nm) seems to be driven by factors with larger spatial and temporal scales – the temporal scale of hours, the spatial scale of few kilometers (<ca. 6 km, i.e. the distance between the urban background sites S1 and S6 here considered, cf. Fig. 1). Nucleation mode particles in the size range >10 nm apparently have the largest spatial scale varying from few kilometers (>6 km, i.e. including all urban sites) to more than 50 km (i.e. including all sites).

5.3 “Paradigm” of spatio-temporal variability of urban aerosol particles

The observed PNSD variations in space and time reflect obviously several processes, such as aerosol dynamics, meteorological changes, mixing and dilution with clean/polluted air, atmospheric chemistry, and proximity to traffic emissions. Their relative contribution is, however, not straightforward to determine.

On one hand, our data show relevant correlations with traffic volume and gaseous compounds (Table 3). The former does not only appear to be a major source of UFPs at the roadside, but also to influence the sub- μm particles in the all region. In addition to the correlation with SO₂, we found at the background sites interesting correlations between the newly formed particles and ozone (and an anti correlation with NO_x and benzene) (cf. Table 3). In fact, ozone is known to be an oxidising agent for VOCs affecting thus the production of condensable organic species (Kulmala et al., 2003). It could have hence been relevant for a “photochemical aging” of new particles up to a certain diameter, and far enough from direct traffic emissions (i.e., PC2, PC4 and PC5 of STA3).

Principal components of particle size distributions

F. Costabile et al.

Title Page

Abstract

Introduction

Conclusions

References

Tables

Figures



Back

Close

Full Screen / Esc

Printer-friendly Version

Interactive Discussion

Principal components of particle size distributionsF. Costabile et al.

[Title Page](#)[Abstract](#)[Introduction](#)[Conclusions](#)[References](#)[Tables](#)[Figures](#)[Back](#)[Close](#)[Full Screen / Esc](#)[Printer-friendly Version](#)[Interactive Discussion](#)

On the other hand, all the PC intra-correlations are ultimately higher than any other observed correlation (cf. Sect. 4.3.3 and Table 3). We interpret this as an argument for the PNSD variability to be primarily governed by intra-dynamic large-scale processes of aerosol aging, in agreement with the aerosol general dynamic equation. A paradigm of urban aerosol evolution is in turn proposed in Fig. 9. It shows the extracted persistent PNSD components in terms of their spatial and temporal variability (or correlations) calculated here.

In summary, in the urban area the larger the diameters, the higher the correlations (and the lower the variability) in both space and time. Notably, when comparing similar diameters, primary particles have lower variability than secondary particles have. Obviously, larger particles appear to scavenge the smaller ones. Less obvious, primary particles seem to reduce the secondary particles with similar diameters, and to increase the particles with larger diameters. Remarkably, the two border lines of the urban aerosol (i.e., the separation urban/regional, and urban/local) are represented by the condensation mode particles on one side, and the fresh nucleation mode particles on the other side. This implies the urban-aged aerosol to be mainly formed by condensation mode particles. It also implies that the fresh nucleation mode particles potentially have in an urban area the highest spatio-temporal variability.

5.4 Implication for exposure and monitoring of ultrafine particles

We here draw some remarks for the exposure and monitoring of UFPs. Notably, the high variance PCs extracted by STA1 (single site) were always parts of the high-variance PCs extracted by the multi-site STAs (cf. Fig. 4 and Fig. 5a). This indicates both the relevance of PNSD large-scale and persistent components, and the difficulty to analyze them by monitoring at a single site alone. This finding also suggests that multiple observation sites are needed even to characterise the PNSD variability at a single site (i.e., all its principal components). We found, indeed, that (cf. Sect. 4.4 and Fig. 7a) traffic sites are poorly representative of Aitken and condensation mode particles, too masked by local emissions. We also found that the pure secondary Aitken

mode particles (i.e. rural Aitken) are inadequately measured in the urban area. This is not the case for the droplet mode particles whereof all sites are equally representative. Hence, the characterization of all persistent and large-scale components of PNSD urban variability seems to require a minimum of four observation sites: one roadside, two urban background, and one rural (cf. STA4). (Obvious, this is expected for an urban area with no local industrial sources.) In fact, the Aitken and accumulation mode components were found to require only three representative sites (roadside, urban background, and rural, cf. STA3). However, we speculate that both the “traffic” and “urban” nucleation mode components require more than the three urban measurement spots (down to 3 nm) used in this study (cf. STA4).

6 Conclusions

Number size distributions of atmospheric aerosol particles (maximum size range 3–800 nm) were measured simultaneously at a maximum of eight observation sites in and around a city in Central Europe (Leipzig, Germany) during two main experiments (2 years at 3 sites; 1 month at 7 sites).

A general observation was that the particle number size distribution varies in time and space in a complex fashion as a result of interaction between local and far-range sources, and the meteorological conditions. To identify statistically independent factors in the urban aerosol, a principal component analysis was conducted encompassing aerosol, gas phase, and meteorological parameters from the multiple sites. Several of the resulting principal components, outstanding with respect to their temporal persistence and spatial coverage, could be associated with aerosol particle modes. Their analysis yielded a surprising wealth of statistical aerosol components occurring in the urban atmosphere over one single city. Meanwhile, satisfactory physical explanations could be found for the components with the greatest temporal persistence and spatial coverage.

A first accumulation mode (“droplet mode”, 300–800 nm) is considered to be the

Principal components of particle size distributions

F. Costabile et al.

Title Page

Abstract

Introduction

Conclusions

References

Tables

Figures



Back

Close

Full Screen / Esc

Printer-friendly Version

Interactive Discussion



result of liquid phase processes and far-range transport. A second accumulation mode (“condensation mode”, 90–250 nm) is considered to represent urban aerosols resulting from primary emissions as well as aging through condensation and coagulation.

The Aitken mode (30–90 nm) is split-up in an urban and a rural component. The urban one has a spatial scale as large as the all city resulting from the interaction of primary and secondary sources. It is more persistent in time and with larger mode diameters than the rural one.

The nucleation mode could be broken down into three size intervals corresponding to different behaviors: <5 nm, 3–20 nm, and >10 nm. The larger the diameters, the higher the spatio-temporal correlations. The 3–20 nm could be separated in further components: traffic type (4–20 nm) linked to the atmospheric processing of primary emissions, and urban and rural types (3–15 and 5–20 nm) linked to photochemically induced particle formation in the urban and rural area, respectively.

Even if these PCs are not truly Lagrangian in that one always follows the other in time, their analysis could help in understanding the aerosol evolution in a Lagrangian perspective. A paradigm on the behaviour of sub- μm urban aerosol particles is in turn proposed, showing the urban PNSD to be primarily governed by intra-dynamic processes of aerosol aging with a larger scale. Based on the results of the study, recommendations can be drawn on how many measurement sites are necessary to monitor individual aerosol components across the entire area of a city.

This study provides information on both, the overall spatial variation of particle number size distributions in an urban area, and the occurring inter-site correlations, which might be useful for particle exposure assessment, atmospheric process identification, and for the validation of numerical models describing aerosol emission, formation, and transport.

Acknowledgements. The PURAT project (Particles in the urban atmosphere: behaviour of fine and ultrafine particles, their spatial variation and relationships with local policy action) was supported by the EU Marie Curie Reintegration Grant FP6-2002-Mobility-11 contract No. 510583. We also thank D. Bake, German Federal Environment Agency (UBA), for his broad

Principal components of particle size distributions

F. Costabile et al.

Title Page

Abstract

Introduction

Conclusions

References

Tables

Figures

⏪

⏩

◀

▶

Back

Close

Full Screen / Esc

Printer-friendly Version

Interactive Discussion

support within the UFOPLAN contract 20442204/03. Assistance with measurements: K. Lupa, K. Stopfkuchen, M. Merkel (IfT) and M. Schilde (UFZ). Measurement data at the sites L1–4 were kindly provided by U. König, Sächsisches Landesamt für Umwelt und Geologie (Saxonian Office for the Environment and Geology, Dresden, Germany). Figure 1 was kindly prepared by R. Otto, student at IfT and the Institute of Geography, University of Leipzig. We also thank J. Heseman for his precious help. Finally, the generous support of I. Allegrini (CNR-IIA) is gratefully acknowledged.

References

- Andronache, C.: Precipitation removal of ultrafine aerosol particles from the atmospheric boundary layer, *J. Geophys. Res.*, 109, D16S07, doi:10.1029/2003JD004050, 2004. 18180
- Birmili, W., Stratmann, F., and Wiedensohler, A.: Design of a DMA-Based Size Spectrometer for a Large Particle Size Range and Stable Operation, *J. Aerosol Sci.*, 30, 549–553, 1999. 18163
- Birmili, W. and Wiedensohler, A.: New particle formation in the continental boundary layer: Meteorological and gas phase parameter influence, *Geophys. Res. Lett.*, 27, 3325–3328, 2000. 18185
- Birmili, W., Wiedensohler, A., Heintzenberg, J., and Lehmann, K.: Atmospheric Particle Number Size Distribution in Central Europe: Statistical Relations to Air Masses and Meteorology, *J. Geophys. Res.*, D23, 32 005–32 018, 2001. 18157
- Birmili, W., Berresheim, H., Plass-Dülmer, C., Elste, T., Gilge, S., Wiedensohler, A., and Uhrner, U.: The Hohenpeissenberg aerosol formation experiment (HAFEX): a long-term study including size-resolved aerosol, H₂SO₄, OH, and monoterpenes measurements, *Atmos. Chem. Phys.*, 3, 361–376, 2003, <http://www.atmos-chem-phys.net/3/361/2003/>. 18185
- Brock, C. A., Trainer, M., Ryerson, T. B., Neuman, J. A., Parrish, D. D., Holloway, J. S., Nicks, D. K. J., Frost, G. J., Hübler, G., and Fehsenfeld, F. C.: Particle growth in plumes of coal-fired power plants, *J. Geophys. Res.*, 107, 4155, doi:10.1029/2001JD001062, 2002. 18184
- Bukowiecki, N., Dommen, J., Prévôt, A. S. H., Weingartner, E., and Baltensperger, U.: Fine and ultrafine particles in the Zrich (Switzerland) area measured with a mobile laboratory: an assessment of the seasonal and regional variation throughout a year, *Atmos. Chem. Phys.*,

Principal components of particle size distributions

F. Costabile et al.

Title Page

Abstract

Introduction

Conclusions

References

Tables

Figures



Back

Close

Full Screen / Esc

Printer-friendly Version

Interactive Discussion

3, 1477–1494, 2003,

<http://www.atmos-chem-phys.net/3/1477/2003/>. 18159

Chan, T. W. and Mozurkewich, M.: Simplified representation of atmospheric aerosol size distributions using absolute principal component analysis, *Atmos. Chem. Phys.* 7, 875–886, 2007.

18163, 18165, 18179, 18184

Doyle, G. J.: Self-nucleation in the sulfuric acid-water system, *J. Chem. Phys.*, 35, 795–799, 1961. 18184

Drewnick F., J. T. Jayne, M. R. Canagaratna, D. R. Worsnop, and Demerjian, K. L.: Measurement of Ambient Aerosol Composition During the PMTACS-NY 2001 Using an Aerosol Mass Spectrometer. Part I: Mass Concentrations, *Aerosol Sci. Tech.*, 38(S1), 92-103, 2004. 18181

Ebert, M., Weinbruch, S., Hoffmann, P., and Ortner, H. M.: The chemical composition and complex refractive index of rural and urban influenced aerosols determined by individual particle analysis, *Atmos. Environ.*, 38, 6531–6545, 2004. 18158

Eder, B. K.: A principal component analysis of SO₄ precipitation concentrations over the eastern United States, *Atmos. Environ.*, 23, 2739–2750, 1989. 18165

Engler, C., Rose, D., Wehner, B., Wiedensohler, A., Brüggemann, E., Gnauk, T., Spindler, G., Tuch, T., and Birmili, W.: Size distributions of non-volatile particle residuals (D_p < 800 nm) at a rural site in Germany and relation to air mass origin, *Atmos. Chem. Phys.* 7, 5785–5802, 2007. 18162

Gnanadesikan, R.: *Methods for statistical data analysis of multivariate observations.*, New York, John Wiley and Sons, Inc., 1977. 18164, 18178

Haywood, J. M. and Boucher, O.: Estimates of the direct and indirect radiative forcing due to tropospheric aerosols: A review, *Rev. Geophys.* 38, 513–543, 2000. 18157

HEI: Understanding the health effects of components of the particulate matter mix: progress and next steps, Tech. Rep. 4, Health Effects Institute, Boston, MA, 2002. 18157

Heintzenberg, J., Birmili, W., Wiedensohler, A., Nowak, A., and Tuch, T.: Structure, variability and persistence of the submicrometre marine aerosol, *Tellus B*, 56(4), 357–367, 2004. 18158

Hering, S. V. and Friedlander, S. K.: Origins of Sulfur Size Distributions in the Los Angeles Basin, *Atmos. Environ.* 16, 2647–2656, 1982. 18181

Hinds, W. C.: *Aerosol Technology*, 2nd ed., John Wiley and Sons, New York, 1999. 18180

Huang, S., Rahn, K. A., and Arimoto, R.: Testing and optimizing two factor-analysis techniques on aerosol at Narragansett, Rhode Island, *Atmos. Environ.*, 33, 2169–2185, 1999. 18163

Hussein, T., Puustinen, A., Aalto, P., Mäkelä, J., Hämeri, K., and Kulmala, M.: Urban aerosol

ACPD

8, 18155–18217, 2008

Principal components of particle size distributions

F. Costabile et al.

Title Page

Abstract

Introduction

Conclusions

References

Tables

Figures

⏪

⏩

◀

▶

Back

Close

Full Screen / Esc

Printer-friendly Version

Interactive Discussion

number size distributions, *Atmos. Chem. Phys.*, 4, 391–411, 2004,
<http://www.atmos-chem-phys.net/4/391/2004/>. 18158

Hussein, T., Hämeri, K., Aalto, P., Paatero, P., and Kulmala, M.: Modal structure and spatial-temporal variations of urban and suburban aerosols in Helsinki, Finland, *Atmos. Environ.*, 39, 1655–1668, 2005. 18158, 18180

Jaenicke, R.: Tropospheric aerosols, in: *Aerosol-cloud-climate interactions*, edited by: Hobbs, P. V., Academic Press, San Diego, CA, 1–31, 1993. 18158

Jimenez, J. L., Jayne, J. T., Shi, Q., Kolb, C. E., Worsnop, D. R., Yourshaw, I., Seinfeld, J. H., Flagan, R. C., Zhang, X., Smith, K. A., Morris, J. W., and Davidovits, P.: Ambient aerosol sampling with an Aerosol Mass Spectrometer, *J. Geophys. Res.*, 108(D7), 8425, doi:10.1029/2001JD001213, 2003. 18181

John, W., Wall, S. M., Ondo, J. L., and Winklmayr, W.: Modes in the size distributions of atmospheric inorganic aerosol, *Atmos. Environ.*, 24A, 2349–2359, 1990. 18174, 18181

John, W.: The characteristics of environmental and laboratory-generated aerosols, in: *Aerosol measurement: Principles, techniques and applications*, edited by: Willeke, K. and Baron, P. A., Van Nostrand Reinhold, New York, 1993. 18158

Jobson, B. T., Parrish, D. D., Goldan, P., Kuster, W., Fehsenfeld, F. C., Blake, D. R., Blake, N. J., and Niki, H.: Spatial and temporal variability of nonmethane hydrocarbon mixing ratios and their relation to photochemical lifetime, *J. Geophys. Res. A*, 103, 13 557–13 567, 1998. 18179

Junge, C. E.: Residence time and variability of tropospheric trace gases, *Tellus*, 16, 477–488, 1974. 18179

Kerminen, V. M. and Wexler, A. S.: The occurrence of sulfuric acid-water nucleation in plumes: Urban environment, *Tellus*, 48B, 6582, 1996. 18184

Ketzel, M. P., Wahlin, A., Kristensson, E., Swietlicki, R., Berkowicz, O. J., Nielsen, and Palmgren, F.: Particle size distribution and particle mass measurements at urban, near-city and rural level in the Copenhagen area and Southern Sweden, *Atmos. Chem. Phys.*, 4, 281–292, 2004,
<http://www.atmos-chem-phys.net/4/281/2004/>. 18159, 18180

Kittelson, D.: Engines and Nanoparticles: A Review, *J. Aerosol Sci.*, 29, 575–588, 1998. 18183

Kulmala, M., Suni, T., Lehtinen, K. E. J., Dal Maso, M., Boy, M., Reissell, A., Rannik, U., Aalto, P., Keronen, P., Hakola, H., Bačk, J., Hoffmann, T., Vesala T., and Hari, P.: A new feedback mechanism linking forests, aerosols, and climate, *Atmos. Chem. Phys.*, 3, 6093–6107, 2003,

Principal components of particle size distributions

F. Costabile et al.

Title Page

Abstract

Introduction

Conclusions

References

Tables

Figures

◀

▶

◀

▶

Back

Close

Full Screen / Esc

Printer-friendly Version

Interactive Discussion

<http://www.atmos-chem-phys.net/3/6093/2003/>. 18185

Kulmala, M., Vehkamäki, H., Petäjä, T., Dal Maso, M., Lauri, A., Kerminen, V. M., Birmili, W., and McMurry, P. H.: Formation and growth rates of ultrafine atmospheric particles: A review of observations, *J. Aerosol Sci.*, 35, 143–176, 2004. 18158

Mäkelä, J. M., Dal Maso, M., Laaksonen, A., Kulmala, M., Pirjola, L., Keronen, P., and Laakso, L.: Characteristics of the aerosol particle formation events observed at a boreal forest site in southern Finland, *Boreal Environ. Res.*, 5, 299–313, 2000. 18157

McFiggans, G., Alfarra, M. R., Allan, J., Bower, K., Coe, H., Cubison, M., Topping, D., Williams, P., Decesari, S., Facchini, C., and Fuzzi, S.: Simplification of the representation of the organic component of atmospheric particulates, *Faraday Discuss.*, 130, 341–362, 2005. 18181

Mejia J. F., Morawska L., and Mengersen, K.: Spatial variation in particle number size distributions in a large metropolitan area, *Atmos. Chem. Phys.*, 8, 1127–1138, 2008, <http://www.atmos-chem-phys.net/8/1127/2008/>. 18180

Meng, Z. and Seinfeld, J. H.: On the source of the submicrometer droplet mode of urban and regional aerosols, *Aerosol Sci. Technol.*, 20, 253–265, 1994. 18174, 18181

Morawska, L., Keogh, D. U., Thomas, S. B., and Mengersen, K.: Modality in ambient particle size distributions and its potential as a basis for developing air quality regulation, *Atmos. Environ.*, 42, 1617–1628, 2008. 18158

Morrison, D. F.: *Multivariate statistical methods*, 2nd ed., McGraw-Hill, New York, 1976. 18164, 18178

Mulaik, S. A.: *The foundations of factor analysis*, McGraw-Hill, New York, 1972. 18164, 18178

Oberdörster, G.: Nanotoxicology: An emerging discipline evolving from studies of ultrafine particles, *Environ. Health Persp.*, 113(7), 823–839, 2005. 18157

Ondov, J. M. and Wexler, A. S.: Where Do Particulate Toxins Reside? An Improved Paradigm for the Structure and Dynamics of the Urban Mid-Atlantic Aerosol, *Environ. Sci. Technol.*, 32, 17, 2547–2555, 1998. 18157

Pope, C. A., Burnett, R. T., Thun, M. J., et al.: Lung cancer, cardiopulmonary mortality, and long-term exposure to fine particulate air pollution, *J. Aerosol Med.*, 287, 1132–1141, 2002. 18157

Pugatshova, A., Reinart, A., and Tamm, E.: Features of the multimodal aerosol size distribution depending on the air mass origin in the Baltic region, *Atmos. Environ.*, 41, 4408–4422, 2007. 18165

Puustinen, A., Hämeri, K., Pekkanen, J., Kulmala, M., Hartog, J., de Meliefste, K., Brink, H.,

Principal components of particle size distributions

F. Costabile et al.

Title Page

Abstract

Introduction

Conclusions

References

Tables

Figures

◀

▶

◀

▶

Back

Close

Full Screen / Esc

Printer-friendly Version

Interactive Discussion

Principal components of particle size distributionsF. Costabile et al.

[Title Page](#)[Abstract](#)[Introduction](#)[Conclusions](#)[References](#)[Tables](#)[Figures](#)[⏪](#)[⏩](#)[◀](#)[▶](#)[Back](#)[Close](#)[Full Screen / Esc](#)[Printer-friendly Version](#)[Interactive Discussion](#)

Kos, G. T., Katsouyanni, K., Karakatsani, A., Kotronarou, A., Kavouras, I., Meddings, C., Thomas, S., Harrison, R., Ayres, J., Zee, S. C., Der, V., and Hoek, G.: Spatial variation of particle number and mass over four European cities, *Atmos. Environ.*, 41, 6622–6636, 2007. 18158, 18180

5 Ramanathan, V., Crutzen, P. J., Kiehl, J. T., and Rosenfeld, D.: Aerosol, climate, and the hydrological cycle, *Science*, 294, 2119–2124, 2001. 18157

Seinfeld, J. H. and Pandis, S. P.: *Atmospheric Chemistry and Physics*, 2nd ed., John Wiley, New York, 2006. 18174, 18180, 18181

10 Sioutas, C., Delfino, R. J., and Singh, M.: Exposure assessment for atmospheric ultrafine particles (UFP) and implications in epidemiological research, *Environ. Health Persp.*, 113(8), 947–955, 2005. 18158, 18184

Stott, P. A., Tett, S. F. B., Jones, G. S., Allen, M. R., Mitchell, J. F. B., and Jenkins, G. J.: External control of 20th century temperature by natural and anthropogenic forcings, *Science*, 290, 2133–2137, 2000. 18157

15 Tuch, T., Herbarth, O., Franck, U., Peters, A., Wehner, B., Wiedensohler, A., and Heintzenberg, J.: Weak correlation of ultrafine aerosol particle concentrations <800 nm between two sites within one city, *J. Expo. Sci. Env. Epid.*, 16, 486–490, 2006. 18158, 18180

Tunved, P., Ström, J., and Hansson, H. C.: An investigation of processes controlling the evolution of the boundary layer aerosol size distribution properties at the Swedish background station Aspöreten, *Atmos. Chem. Phys.*, 4, 2581–2592, 2004, <http://www.atmos-chem-phys.net/4/2581/2004/>. 18179

20 Voigtländer, J., Tuch, T., Birmili, W., and Wiedensohler, A.: Correlation between traffic density and particle size distribution in a street canyon and the dependence on wind direction, *Atmos. Chem. Phys.*, 6, 4275–4286, 2006, <http://www.atmos-chem-phys.net/6/4275/2006/>. 18161

25 Wehner, B., Birmili, W., Gnauk, T., and Wiedensohler, A.: Particle number size distributions in a street canyon and their transformation into the urban background: Measurements and a simple model study, *Atmos. Environ.*, 36, 2215–2223, 2002. 18180

30 Wehner, B., and Wiedensohler, A.: Long term measurements of submicrometer urban aerosols: statistical analysis for correlations with meteorological conditions and trace gases, *Atmos. Chem. Phys.*, 3, 867–879, 2003, <http://www.atmos-chem-phys.net/3/867/2003/>. 18162

Wehner, B., Siebert, H., Stratmann, F., Tuch, T., Wiedensohler, A., Petäjä, T., Dal Maso, M.,

and Kulmala, M.: Horizontal homogeneity and vertical extent of new particle formation events, *Tellus*, 59B, 362–371, 2007. 18183

Whitby, K.T.: The physical characteristics of sulphur aerosols, *Atmos. Environ.*, 12, 135–159, 1978. 18157

- 5 WHO: World Health Report 2002, Tech. Rep., World Health Organisation, Genova, 2002. 18157

ACPD

8, 18155–18217, 2008

**Principal
components of
particle size
distributions**

F. Costabile et al.

Title Page

Abstract

Introduction

Conclusions

References

Tables

Figures

⏪

⏩

◀

▶

Back

Close

Full Screen / Esc

Printer-friendly Version

Interactive Discussion

Principal components of particle size distributions

F. Costabile et al.

Table 1. Description of atmospheric PNSD measurements in Leipzig: **(a)** measurement sites and their characteristics, **(b)** measurement periods during the short-term spatial experiment in 2005 and instrumental parameters. The location of the sites is depicted in Fig. 1.

Site No.	Name	Type	Description	Traffic volume	Inlet height	
(a)	S1	Schleussig	urban background	in a backyard	–	~18 m
	S2	Inselstrasse	urban background	high above a low-trafficked street	–	~18 m
	S3	Listplatz	roadside	near a highly trafficked square	>50 000 veh/day	~10 m
	S4	Rabet	urban background	in a public park	–	~5 m
	S5	Eisenbahnstrasse	roadside	inside a street canyon	>10 000 veh/day	~6 m
	S6	IFT	urban background	on the roof of the institute building	–	~16 m
	S7	Melpitz	rural background	surrounded by pastures	–	~6 m
	S8a–d	mobile	roadside/urban background	variable	variable	~5 m

Site No.	Name	Measurements period	Size spectrometer type	Dp size range	Time resolution	
(b)	S1	Schleussig	18 March–31 May	Twin DMPS–IFT	3–800 nm	10 min
	S2	Inselstrasse	7 April–9 May	SMPS–TSI 8085	10–500 nm	6 min
	S3	Listplatz	29 March–9 May	SMPS–IFT	10–900 nm	6 min
	S4	Rabet	23 March–17 May	SMPS–IFT	10–900 nm	6 min
	S5	Eisenbahnstrasse	1 March–31 May	Twin DMPS–IFT	3–800 nm	20 min
	S6	IFT	1 March–31 May	Twin DMPS–IFT	3–800 nm	20 min
	S7	Melpitz	1 March–31 May	Twin DMPS–IFT	3–800 nm	20 min
	S8a–d	mobile	7 April–27 May	SMPS–TSI 8085	10–500 nm	6 min

Title Page

Abstract

Introduction

Conclusions

References

Tables

Figures

◀

▶

◀

▶

Back

Close

Full Screen / Esc

Printer-friendly Version

Interactive Discussion

Principal components of particle size distributions

F. Costabile et al.

Table 2. Description of the 5 multivariate analyses (STA1, STA3, STA4, STA6, and STA7) presented in this work. In “STA/” the index indicates the number of sites included in each principal component analysis.

Name	Observation sites used	Measurement duration	Measurement period	Particle size range	Comment
STA1	S5–S7	2 years	2005 & 2006	3–800 nm	3 sites individually, long-term
STA3	S5–S7	2 years	2005 & 2006	3–800 nm	3 sites combined, long-term
STA4	S1, S5–S7	70 days	March–May 2005	3–800 nm	4 sites combined, wide size range
STA6	S1–S6	33 days	April–May 2005	10–470 nm	6 urban sites combined, limited size range
STA7	S1–S7	17 days	April 2005	10–470 nm	7 sites combined, largest spatial coverage

Title Page

Abstract

Introduction

Conclusions

References

Tables

Figures

⏪

⏩

◀

▶

Back

Close

Full Screen / Esc

Printer-friendly Version

Interactive Discussion

Principal components of particle size distributions

F. Costabile et al.

Title Page

Abstract

Introduction

Conclusions

References

Tables

Figures

◀

▶

◀

▶

Back

Close

Full Screen / Esc

Printer-friendly Version

Interactive Discussion



Table 3. Principal components in the atmospheric PNSD: characteristics and correlations.

Type ¹	Description	Modal size range ² (nm)	Likely sources	Spatial scale	Sites predominantly affected ³	Temporal scale and characteristics	Intra correlations ^{4,5}	Inter correlations ^{4,5,6}
NM	fresh, roadside	<5	traffic emissions	local	all	hours	urban AkM, urban traffic*, droplet mode*	T, WS, LDV, HDV, NO, NO ₂ , NO _x , P*, RH*
NM	fresh, back-ground	<5	photochemically induced particle formation and traffic	local	all	hours	urban AkM, urban traffic*, droplet mode*	GR, T, LDV, HDV, SO ₂ , NO, NO ₂ , NO _x , CO, benzene, RH*
NM	urban back-ground	3–15	photochemically induced particle formation	local to urban to regional	UB & RB	hours; ↑ at daytime, midday peak, ↑ in summer	NM–rural, urban AkM, urban traffic, droplet mode*, nucleation-traffic*, aged nucleation*	GR, T, MLH, WS, WD, SO ₂ , NO, NO ₂ , NO _x , O ₃ , benzene*, RH*
NM	roadside	4–20	nucleation of emitted gases	local to urban	RS	hours; ↑ at daytime, three daily peaks, weekly cycle, ↑ in summer	aged NM, urban traffic, NM-urban*, NM-rural*	GR, P, T, MLH, WS, WD, LDV, NO, HDV*
NM	rural	5–20	photochemically induced particle formation	local to regional	RB	hours; ↑ at daytime, midday peak, ↑ in summer	nucleation-urban, aged nucleation, urban AkM, rural AkM, droplet mode*, NM-traffic*, urban traffic*	GR, WD, O ₃ , RH*, benzene*, NO _x
NM	aged-urban	10–50	aging of NM particles and traffic emissions	urban to regional	UB & RB	hours; ↑ at daytime, two daily peaks, weekly cycle, higher in summer	NM-rural, NM-urban*, urban AkM*	P, T, LDV, O ₃ , RH*, benzene*, NO _x

Table 3. Continued.

Type ¹	Description	Modal size range ² (nm)	Likely sources	Spatial scale	Sites predominantly affected ³	Temporal scale and characteristics	Intra correlations ^{4,5}	Inter correlations ^{4,5,6}
AkM	urban traffic	30–200	traffic emissions	urban to regional	RS	↑ at daytime, two daily peaks, weekly cycle	condensation mode, NM-traffic, NM-urban, NM-fresh*, NM-aged*, NM-rural*, urban AkM*	T, LDV, HDV
AkM	urban	30–90	aging of NM particles and traffic emissions	urban to regional	UB & RB	<1 day; ↑ at nighttime, ↑ in summer	NM-fresh, condensation mode, rural AkM, urban traffic*, NM-urban*, NM-rural*, urban traffic AkM*	P, RH, LDV, HDV, SO ₂ , benzene, WD, GR*, T*
AkM	rural	20–70	aging of NM particles	local to urban	RB	↑ in the evening, ↑ in summer	urban AkM, NM-urban*, NM-rural*, AcM*	P, O ₃ , WD, benzene*, NO _x *
AcM	–	>200	long range transport	regional	all	–	NM-urban*, NM-rural*	GR, T, PM ₁₀ , WD, SO ₂ , benzene, NO ₂ , RH*, WS*, O ₃ *
AcM	“condensation mode”	90–250	aging of urban particles, traffic	urban to regional	all	<1 day; ↑ in summer	droplet mode, urban traffic	GR, P, T, WD, O ₃ , benzene*, NO _x , RH*
AcM	“droplet mode”	300–800	cloud & fog processing	regional	all	>1 day; ↑ in winter	nucleation-fresh*, LRT	RH, WS, WD, LDV, HDV, GR*, T*

¹NM: nucleation mode, AkM: Aitken mode, AcM: accumulation mode. ²The modal size range was defined as the area around the peak in the curve of the factor loading as a function of particle size, delimited by the positions of 2/3 of the peak value on both sites. ³RB: rural background, UB: urban background, RS: roadside. ⁴Only correlations >0.3 are shown. ⁵The asteriks (*) indicates anti correlation. ⁶RH: relative humidity, T: temperature, GR: global radiation, P: pressure, WS: wind speed, WD: wind direction, LDV: light duty vehicles, HDV: heavy duty vehicles, LRT: long range transport, MLH: mixing layer height.

Principal components of particle size distributions

F. Costabile et al.

Title Page

Abstract

Introduction

Conclusions

References

Tables

Figures

◀

▶

◀

▶

Back

Close

Full Screen / Esc

Printer-friendly Version

Interactive Discussion

Principal components of particle size distributions

F. Costabile et al.

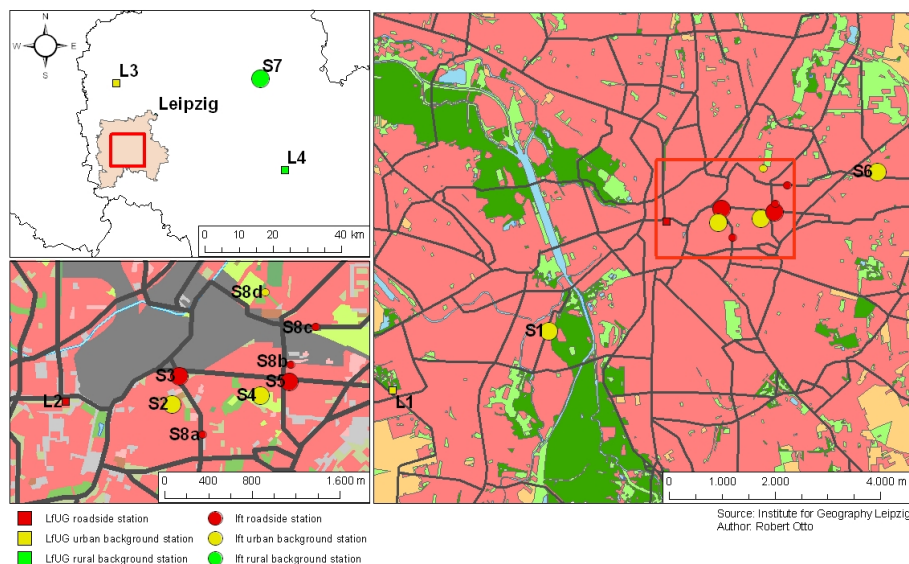


Fig. 1. Location of the atmospheric measurement sites during the experiment. Upper left map: region around the city of Leipzig, Germany, with the three regional background sampling sites S7, L3 and L4. Right map: area of the city of Leipzig including the urban background sampling sites S1, S6, and L1. Lower left map: the main urban area under investigation in eastern Leipzig, including the urban background sites S2, S4, and S8d, and the roadside sites S3, S5, S8a, S8b, S8c, and L2. Insets into the next bigger scale are indicated by red rectangles. The sites S1–8 were operated by IFT whereas the sites L1–4 represent routine observation sites by the Saxonian Office for the Environment and Geology.

[Title Page](#)
[Abstract](#)
[Introduction](#)
[Conclusions](#)
[References](#)
[Tables](#)
[Figures](#)
[◀](#)
[▶](#)
[◀](#)
[▶](#)
[Back](#)
[Close](#)
[Full Screen / Esc](#)
[Printer-friendly Version](#)
[Interactive Discussion](#)

Principal components of particle size distributions

F. Costabile et al.

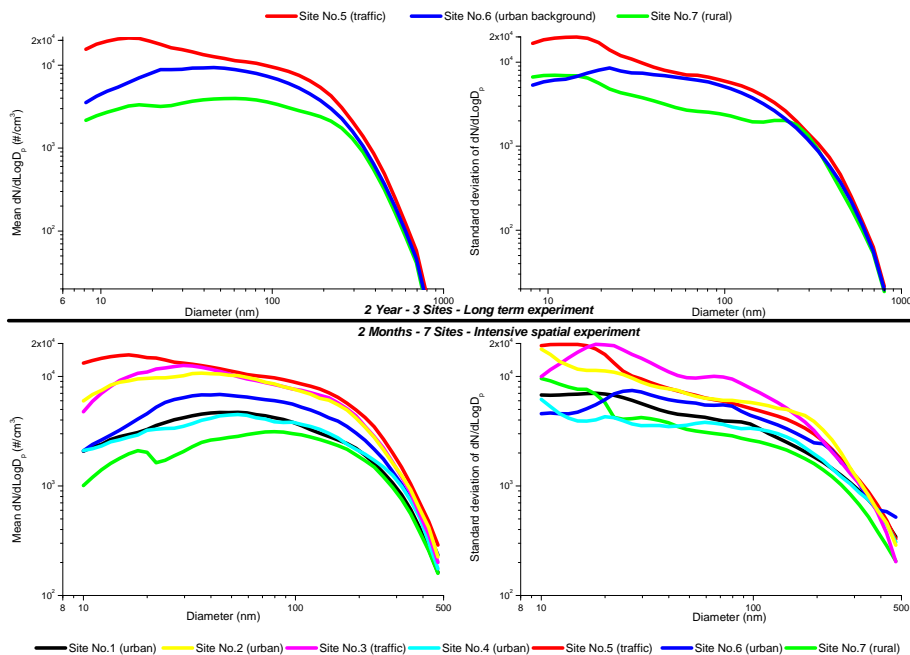


Fig. 2. Average concentrations (left) and standard deviation (right) of the PNSD measured at the sites S5–S7 during the long-term experiment, and at the sites S1–S7 during the intensive spatial experiment.

Title Page

Abstract

Introduction

Conclusions

References

Tables

Figures

◀

▶

◀

▶

Back

Close

Full Screen / Esc

Printer-friendly Version

Interactive Discussion

Principal components of particle size distributions

F. Costabile et al.

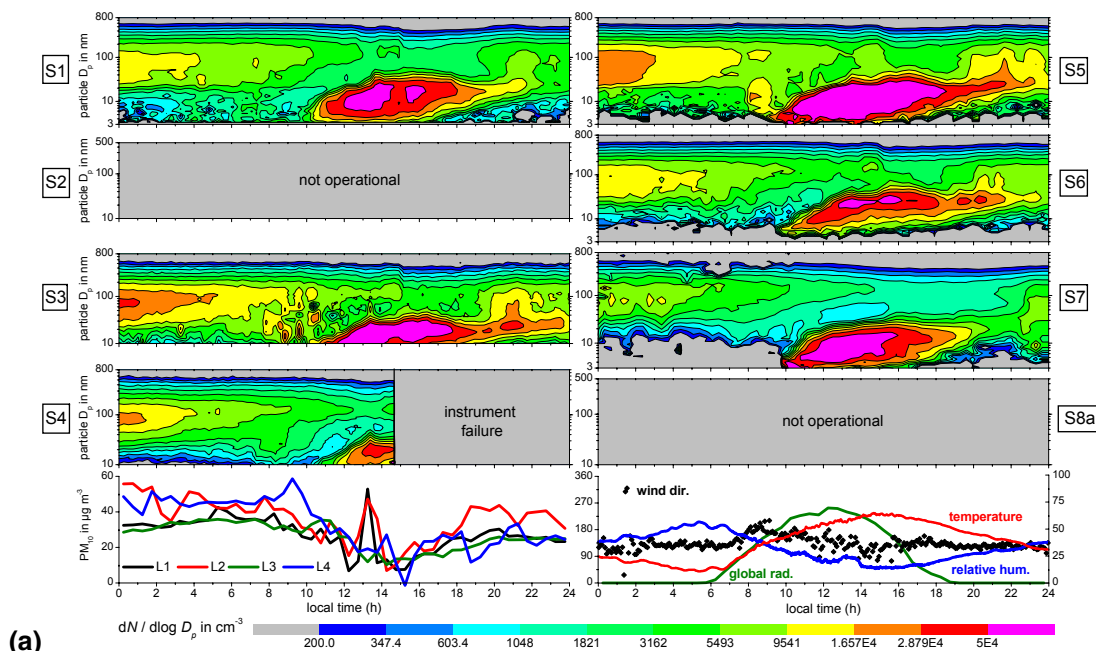


Fig. 3. Particle number size distributions on April 3, 2005 (Sunday), measured simultaneously at 6 sites in Leipzig. PM₁₀ mass concentrations are taken from the LfUG network. Meteorological parameters originate from site S6 except wind direction, which was measured 4 m above the roof-top level of site S5. The scales of the meteorological parameters are: wind direction in 1° (left axis), temperature in 10°C (left axis), global radiation in 10 W m⁻² (right axis), and relative humidity in % (right axis). For the location of the sites, see Fig. 1.

Title Page

Abstract

Introduction

Conclusions

References

Tables

Figures

◀

▶

◀

▶

Back

Close

Full Screen / Esc

Printer-friendly Version

Interactive Discussion

Principal components of particle size distributions

F. Costabile et al.

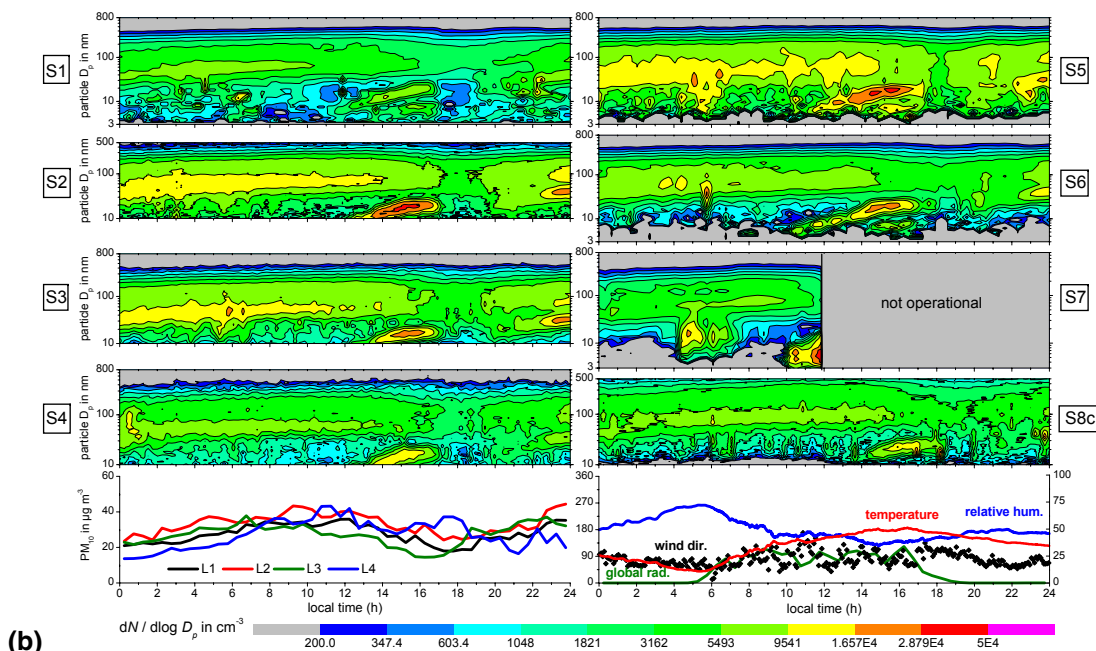


Fig. 3. Particle number size distributions on 24 April 2005 (Sunday), measured simultaneously at 8 sites in Leipzig. PM_{10} mass concentrations are taken from the LfUG network. Meteorological parameters originate from site S6 except wind direction, which was measured 4 m above the roof-top level of site S5. The scales of the meteorological parameters are: wind direction in 1° (left axis), temperature in 10°C (left axis), global radiation in 10 W m^{-2} (right axis), and relative humidity in % (right axis). For the location of the sites, see Fig. 1.

Title Page

Abstract

Introduction

Conclusions

References

Tables

Figures

◀

▶

◀

▶

Back

Close

Full Screen / Esc

Printer-friendly Version

Interactive Discussion

Principal components of particle size distributions

F. Costabile et al.

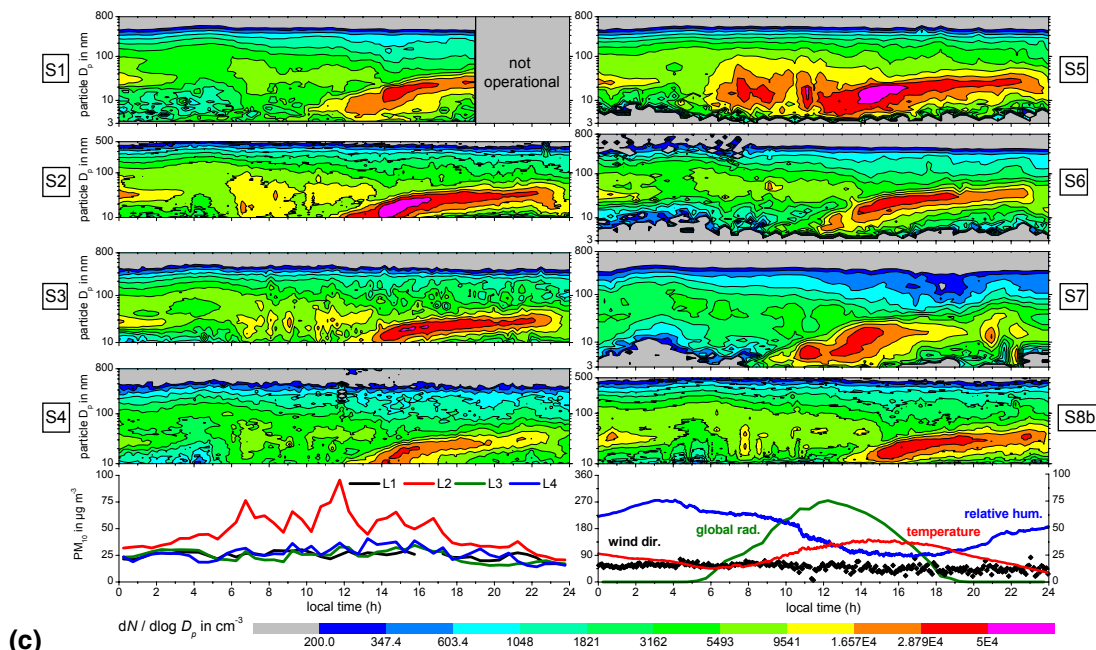


Fig. 3. Particle number size distributions on 20 April 2005 (Wednesday), measured simultaneously at 8 sites in Leipzig. PM_{10} mass concentrations are taken from the LfUG network. Meteorological parameters originate from site S6 except wind direction, which was measured 4 m above the roof-top level of site S5. The scales of the meteorological parameters are: wind direction in 1° (left axis), temperature in 10°C (left axis), global radiation in 10 W m^{-2} (right axis), and relative humidity in % (right axis). For the location of the sites, see Fig. 1.

Title Page

Abstract

Introduction

Conclusions

References

Tables

Figures

◀

▶

◀

▶

Back

Close

Full Screen / Esc

Printer-friendly Version

Interactive Discussion

Principal components of particle size distributions

F. Costabile et al.

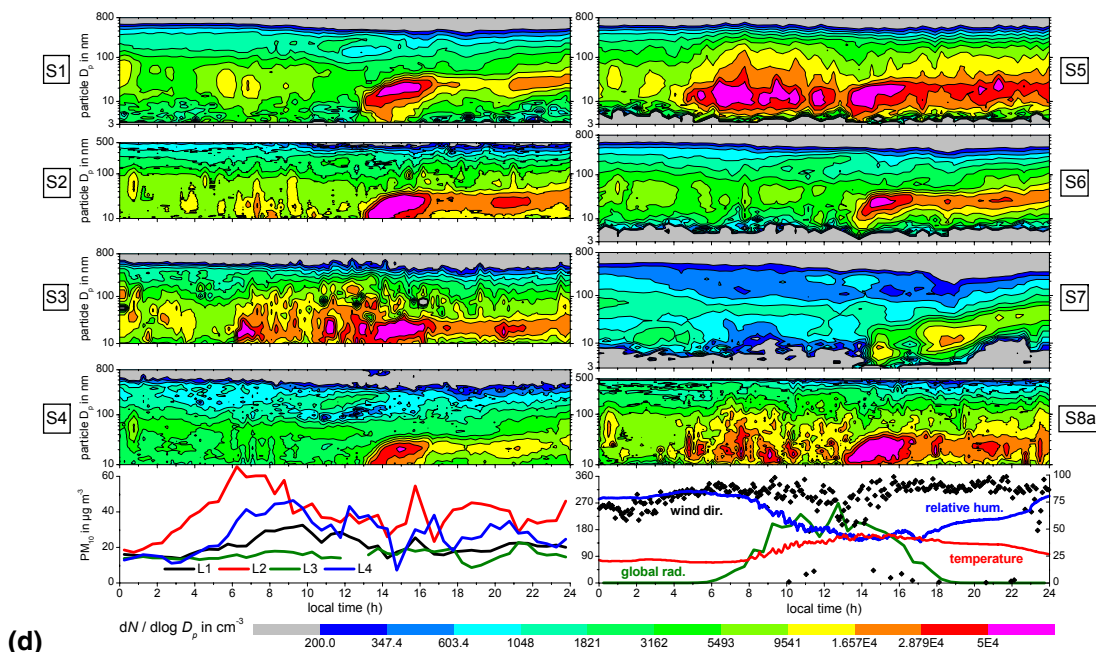


Fig. 3. Particle number size distributions on 11 April 2005 (Monday), measured simultaneously at 8 sites in Leipzig. PM_{10} mass concentrations are taken from the LfUG network. Meteorological parameters originate from site S6 except wind direction, which was measured 4 m above the roof-top level of site S5. The scales of the meteorological parameters are: wind direction in 1° (left axis), temperature in 10°C (left axis), global radiation in 10 W m^{-2} (right axis), and relative humidity in % (right axis). For the location of the sites, see Fig. 1.

Title Page

Abstract

Introduction

Conclusions

References

Tables

Figures

◀

▶

◀

▶

Back

Close

Full Screen / Esc

Printer-friendly Version

Interactive Discussion

Principal components of particle size distributions

F. Costabile et al.

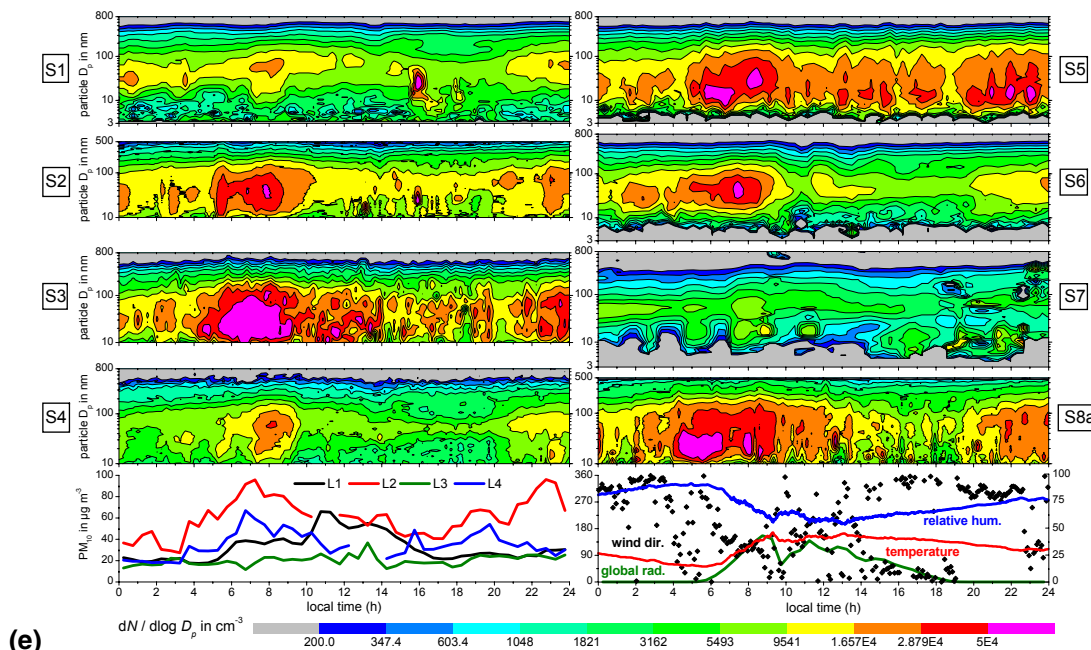


Fig. 3. Particle number size distributions on 12 April 2005 (Tuesday), measured simultaneously at 8 sites in Leipzig. PM_{10} mass concentrations are taken from the LfUG network. Meteorological parameters originate from site S6 except wind direction, which was measured 4 m above the roof-top level of site S5. The scales of the meteorological parameters are: wind direction in 1° (left axis), temperature in 10°C (left axis), global radiation in 10 W m^{-2} (right axis), and relative humidity in % (right axis). For the location of the sites, see Fig. 1.

Title Page

Abstract

Introduction

Conclusions

References

Tables

Figures

◀

▶

◀

▶

Back

Close

Full Screen / Esc

Printer-friendly Version

Interactive Discussion

Principal components of particle size distributions

F. Costabile et al.

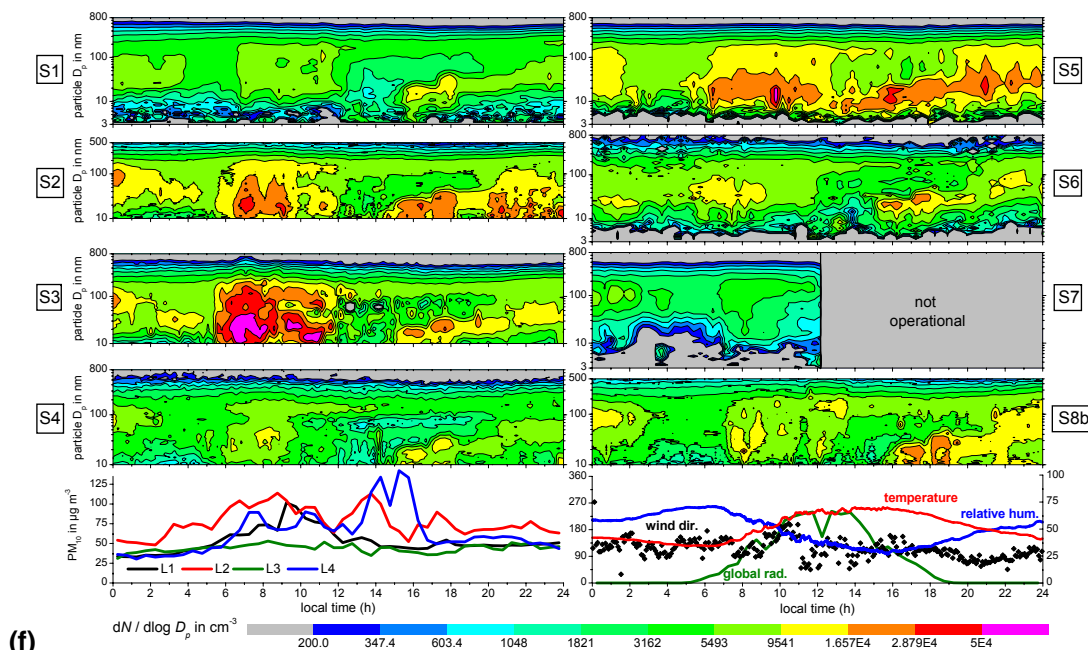


Fig. 3. Particle number size distributions on 15 April 2005 (Friday), measured simultaneously at 8 sites in Leipzig. PM_{10} mass concentrations are taken from the LfUG network. Meteorological parameters originate from site S6 except wind direction, which was measured 4 m above the roof-top level of site S5. The scales of the meteorological parameters are: wind direction in 1° (left axis), temperature in 10°C (left axis), global radiation in 10 W m^{-2} (right axis), and relative humidity in % (right axis). For the location of the sites, see Fig. 1.

Title Page

Abstract

Introduction

Conclusions

References

Tables

Figures

◀

▶

◀

▶

Back

Close

Full Screen / Esc

Printer-friendly Version

Interactive Discussion

Principal components of particle size distributions

F. Costabile et al.

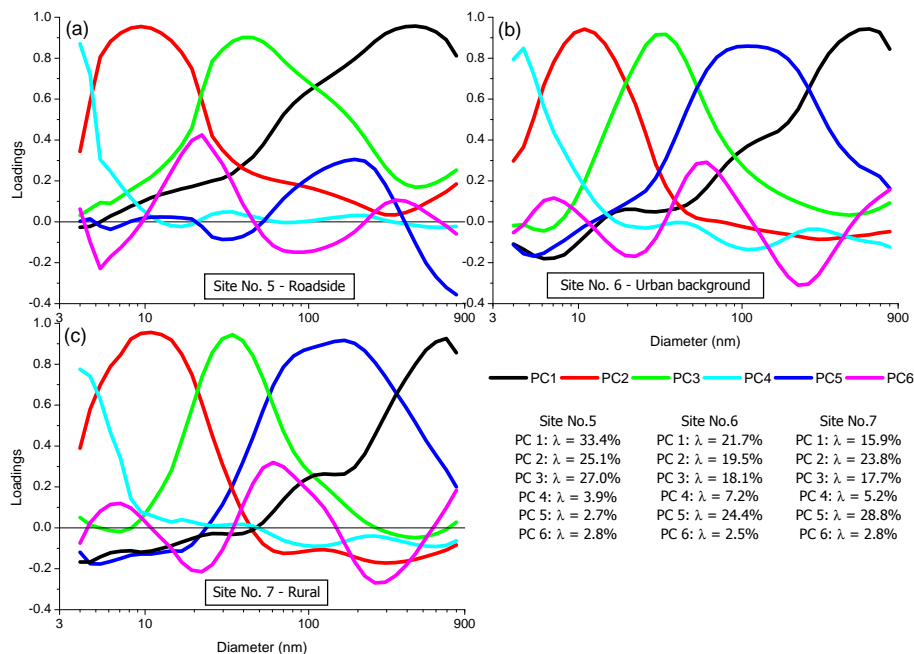


Fig. 4. Results of the principal component analysis STA1, covering the long-term experiment: **(a)** site S5 (roadside), **(b)** site S6 (urban background), and **(c)** site S7 (rural). The variance explained by each component (λ) is given as relative percentage of the total variance.

Title Page

Abstract

Introduction

Conclusions

References

Tables

Figures

◀

▶

◀

▶

Back

Close

Full Screen / Esc

Printer-friendly Version

Interactive Discussion

Principal components of particle size distributions

F. Costabile et al.

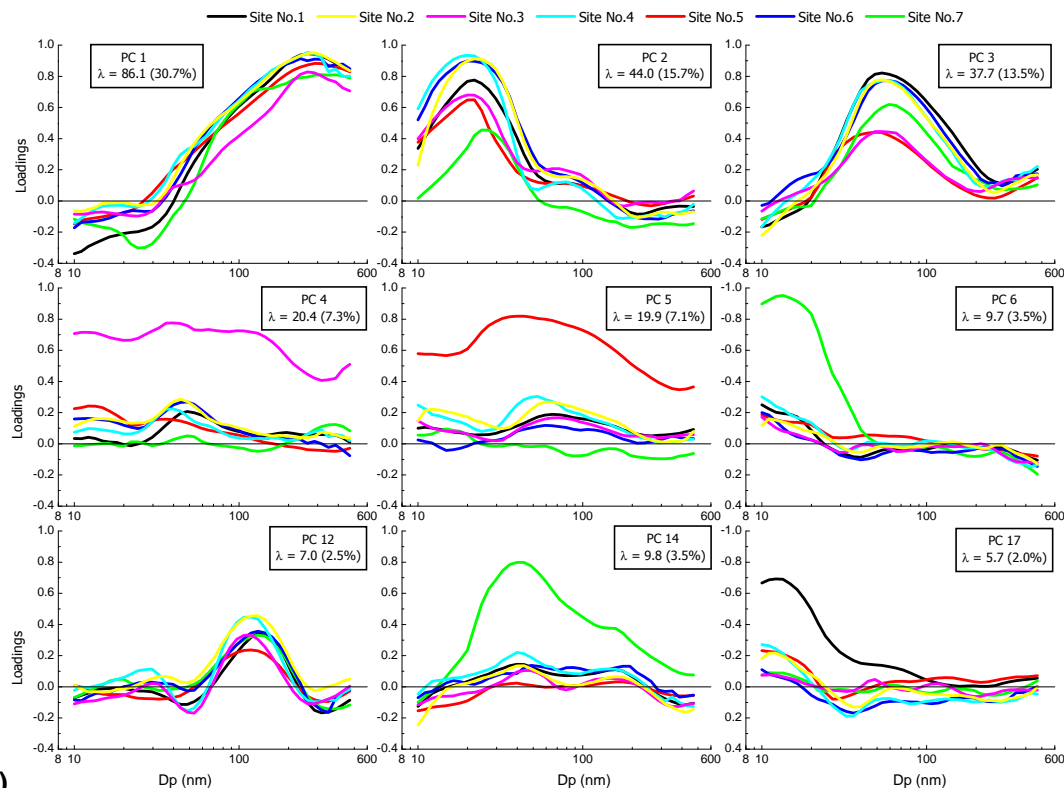


Fig. 5. Factor loadings of the nine most significant principal components (PC) in STA7 (cf. Table 2). Only those PCs are shown whose variance exceed 2.0 % of the variance of the total data set. The variance λ is given for each PC as both eigenvalue and relative percentage. (The number of components and the 2.0 % threshold results from the application of the Kaiser and Scree plot criteria.)

Title Page

Abstract

Introduction

Conclusions

References

Tables

Figures

◀

▶

◀

▶

Back

Close

Full Screen / Esc

Printer-friendly Version

Interactive Discussion

Principal components of particle size distributions

F. Costabile et al.

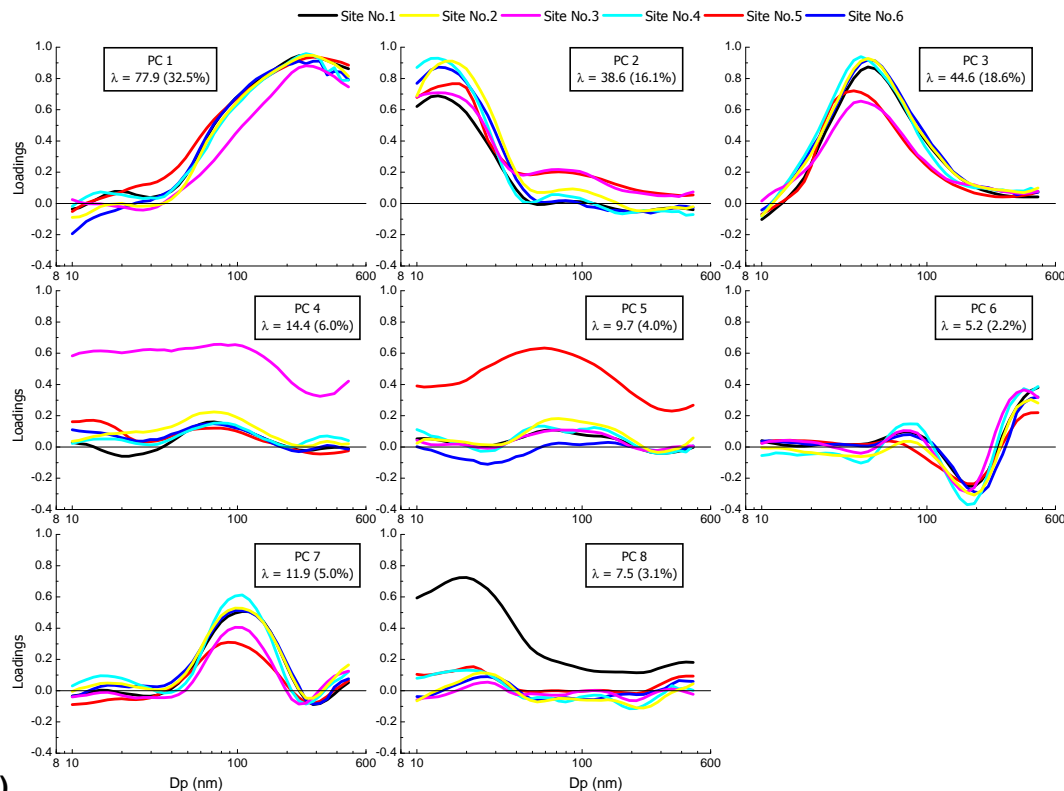
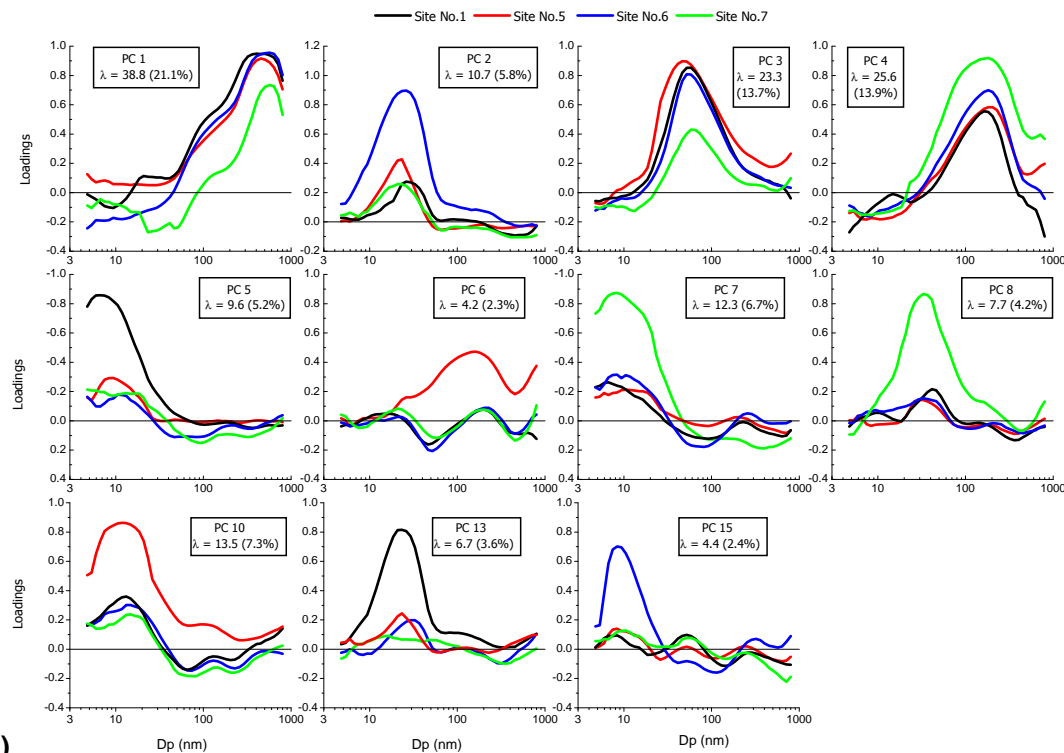


Fig. 5. Factor loadings of 8 most significant principal components (PC) in STA6 (cf. Table 2), i.e. excluding the rural site S7. Only those PCs are shown whose variance exceed 2.2% of the variance of the total data set. The variance λ is given for each PC as both eigenvalue and relative percentage. (The number of components and the 2.2% threshold results from the application of the Kaiser and Scree plot criteria.)

[Title Page](#)[Abstract](#)[Introduction](#)[Conclusions](#)[References](#)[Tables](#)[Figures](#)[◀](#)[▶](#)[◀](#)[▶](#)[Back](#)[Close](#)[Full Screen / Esc](#)[Printer-friendly Version](#)[Interactive Discussion](#)

Principal components of particle size distributions

F. Costabile et al.



(c) Fig. 5. Factor loadings of 11 most significant principal components (PC) in STA4 (cf. Table 2). Only those PCs are shown whose variance exceeded 2.3% of the variance of the total data set. The variance λ is given for each PC as both eigenvalue and relative percentage. (The number of components and the 2.3% threshold results from the application of the Kaiser and Scree plot criteria.)

Title Page

Abstract

Introduction

Conclusions

References

Tables

Figures

◀

▶

◀

▶

Back

Close

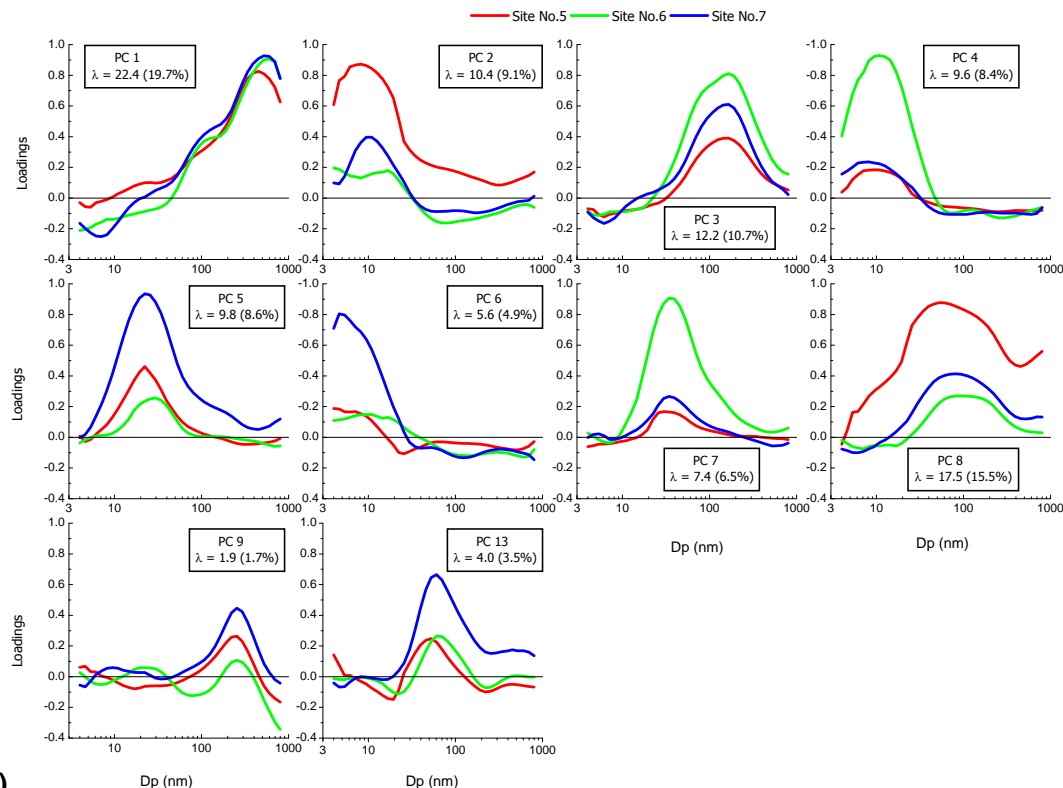
Full Screen / Esc

Printer-friendly Version

Interactive Discussion

Principal components of particle size distributions

F. Costabile et al.



(d) Fig. 5. Factor loadings of 10 most significant principal components (PC) in STA3 (cf. Table 2). Only those PCs are shown whose variance exceed 1.7% of the variance of the total data set. The variance λ is given for each PC as both eigenvalue and relative percentage. (The number of components and the 1.7% threshold results from the application of the Kaiser and Scree plot criteria, as explained in Sect. 3.)

Title Page

Abstract

Introduction

Conclusions

References

Tables

Figures

◀

▶

◀

▶

Back

Close

Full Screen / Esc

Printer-friendly Version

Interactive Discussion

Principal components of particle size distributions

F. Costabile et al.

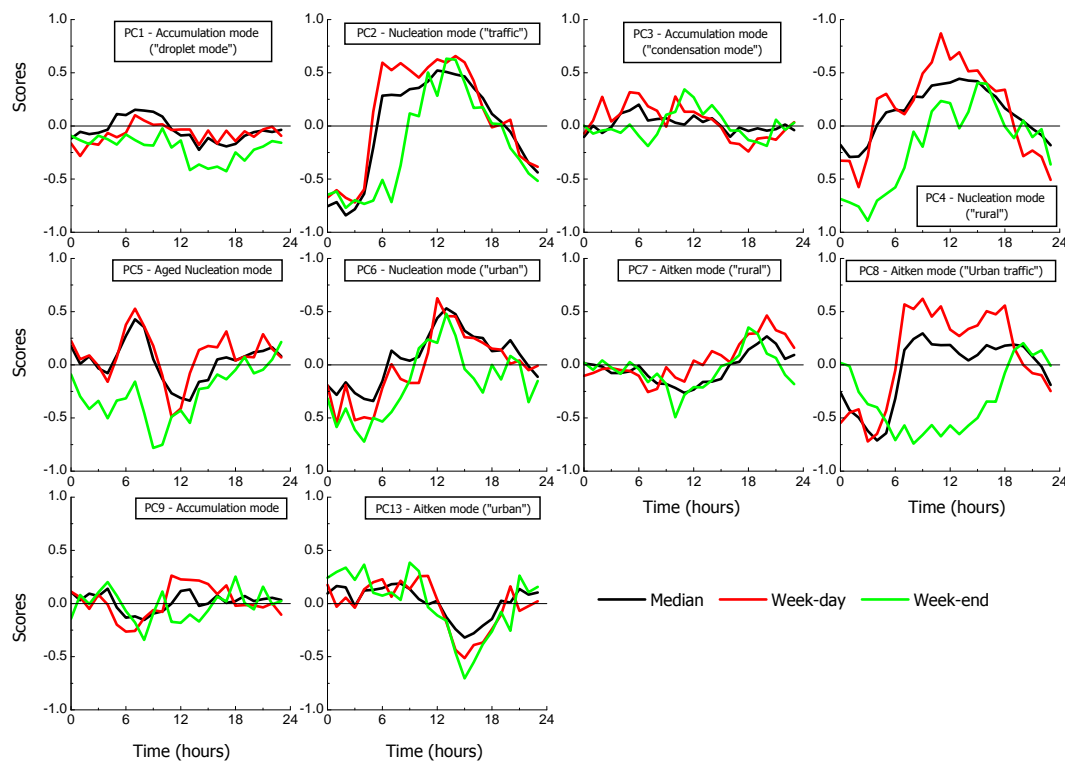


Fig. 6. Diurnal cycles of the principal component scores calculated in STA3 (cf. Table 2). Median values across the entire data set are compared against week-day and week-end average values.

Title Page

Abstract

Introduction

Conclusions

References

Tables

Figures

◀

▶

◀

▶

Back

Close

Full Screen / Esc

Printer-friendly Version

Interactive Discussion

Principal components of particle size distributions

F. Costabile et al.

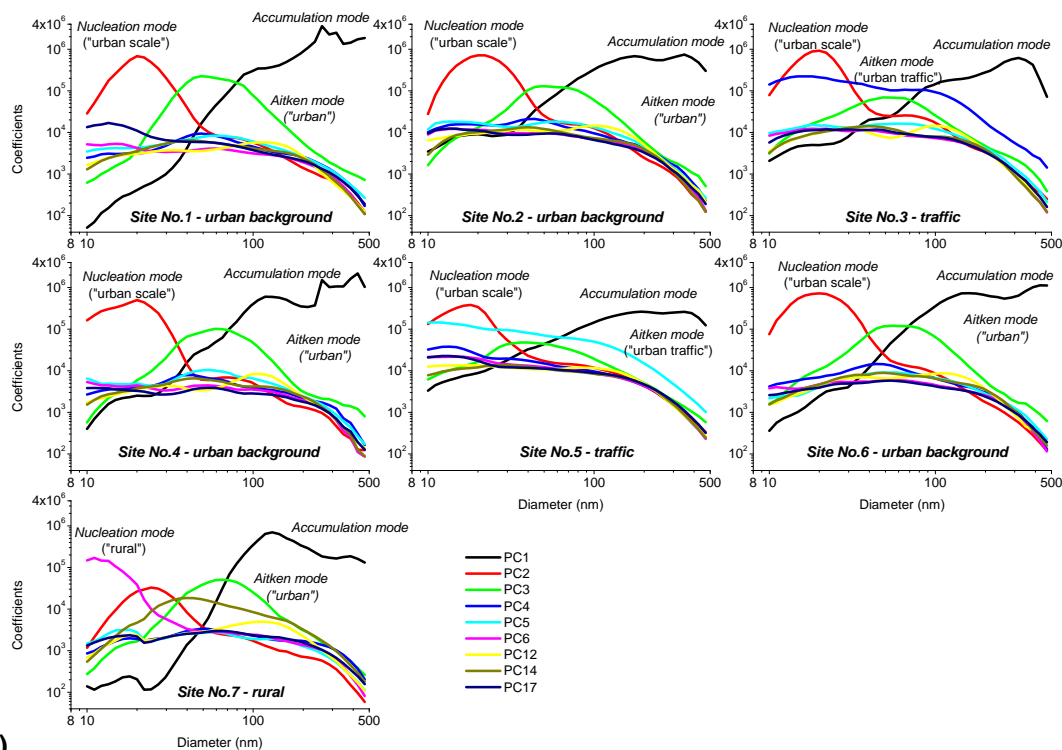


Fig. 7. Signature particle size distributions in STA7 calculated according to the principal component coefficients (cf. Table 2).

Title Page

Abstract

Introduction

Conclusions

References

Tables

Figures

◀

▶

◀

▶

Back

Close

Full Screen / Esc

Printer-friendly Version

Interactive Discussion

Principal components of particle size distributions

F. Costabile et al.

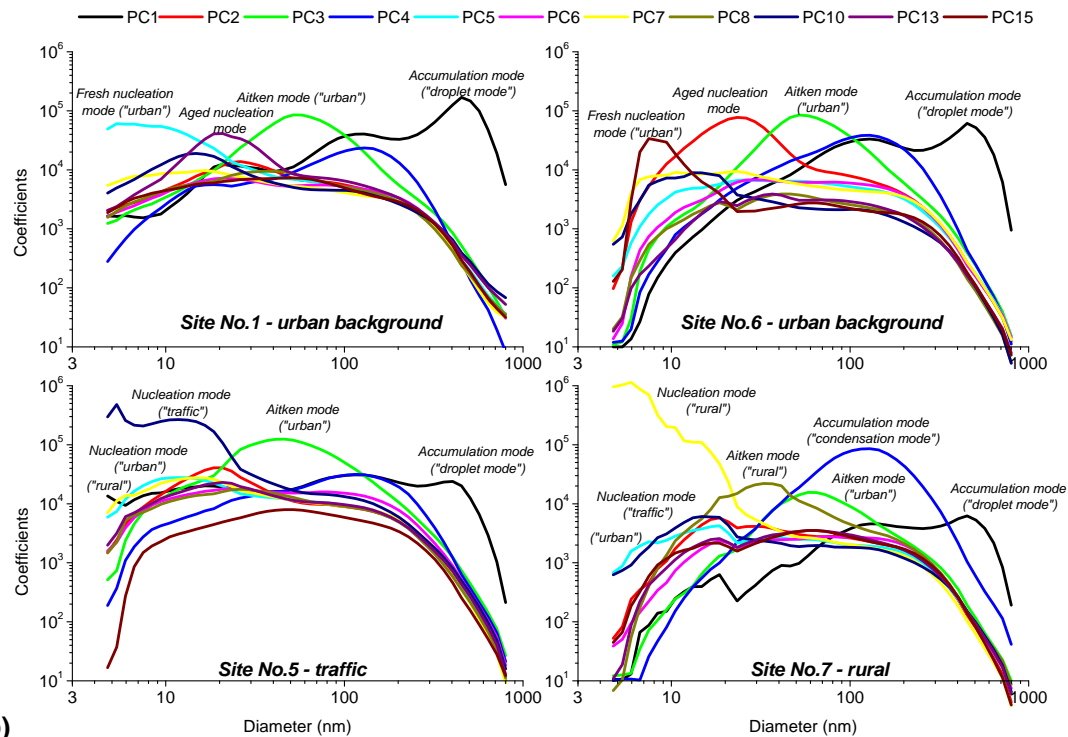


Fig. 7. Signature particle size distributions in STA4 calculated according to the principal component coefficients (cf. Table 2).

Title Page

Abstract

Introduction

Conclusions

References

Tables

Figures

◀

▶

◀

▶

Back

Close

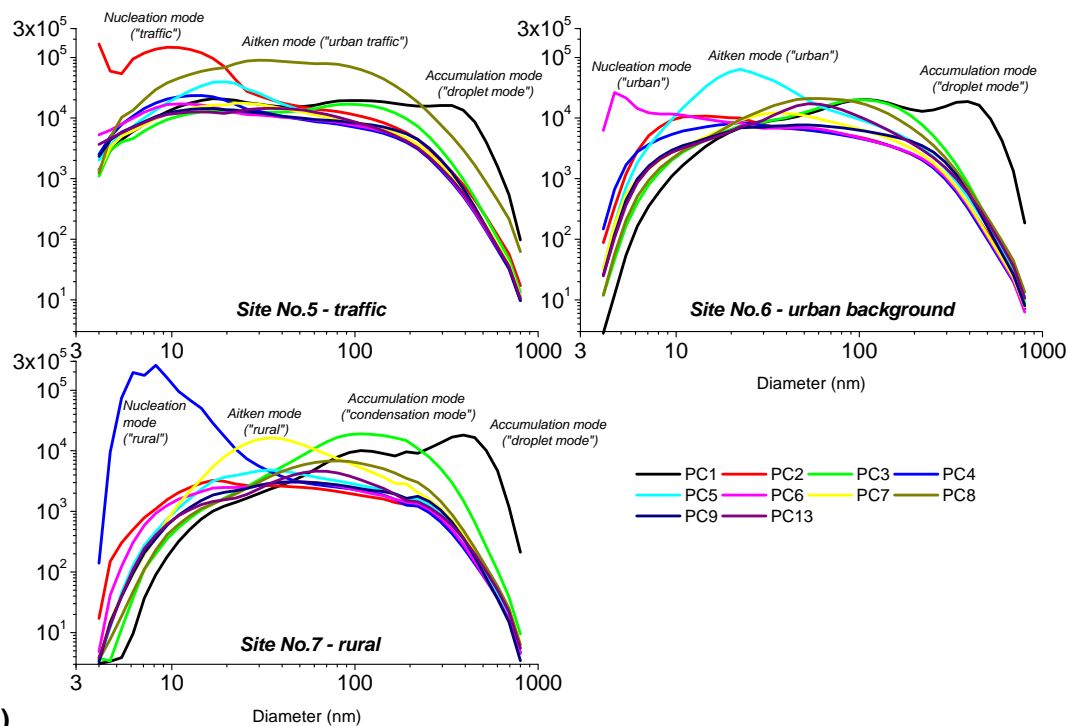
Full Screen / Esc

Printer-friendly Version

Interactive Discussion

Principal components of particle size distributions

F. Costabile et al.



(c) **Fig. 7.** Signature particle size distributions in STA3 calculated according to the principal component coefficients (cf. Table 2).

Title Page

Abstract

Introduction

Conclusions

References

Tables

Figures

◀

▶

◀

▶

Back

Close

Full Screen / Esc

Printer-friendly Version

Interactive Discussion

Principal components of particle size distributions

F. Costabile et al.

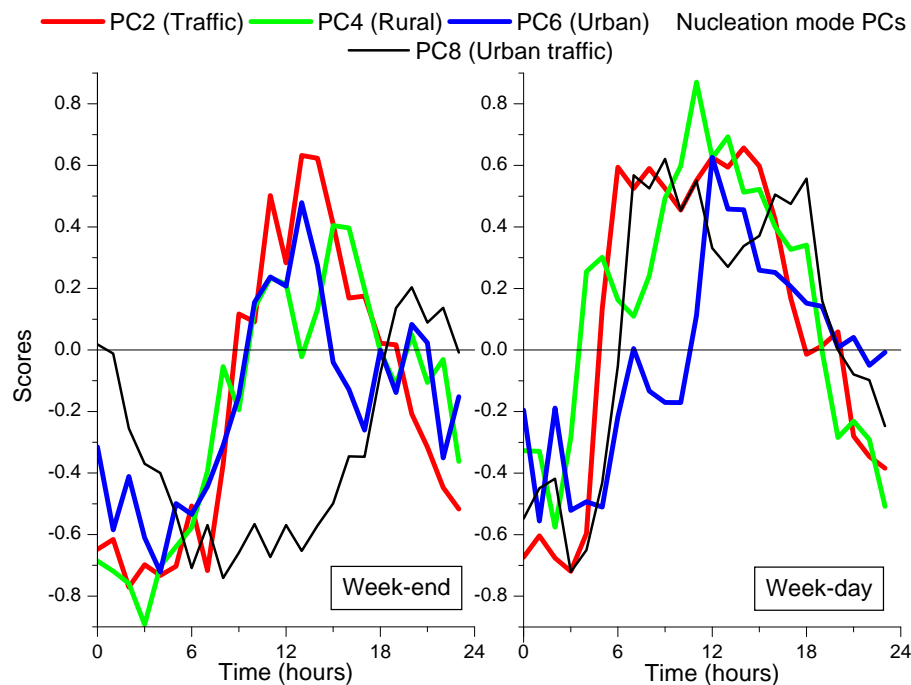


Fig. 8. Week-end and week-day mean diurnal cycles of the scores of the nucleation modes PC2, PC4, and PC6, and the urban traffic PC8 extracted in STA3 (cf. Tab. 2).

[Title Page](#)[Abstract](#)[Introduction](#)[Conclusions](#)[References](#)[Tables](#)[Figures](#)[◀](#)[▶](#)[◀](#)[▶](#)[Back](#)[Close](#)[Full Screen / Esc](#)[Printer-friendly Version](#)[Interactive Discussion](#)

Principal components of particle size distributions

F. Costabile et al.

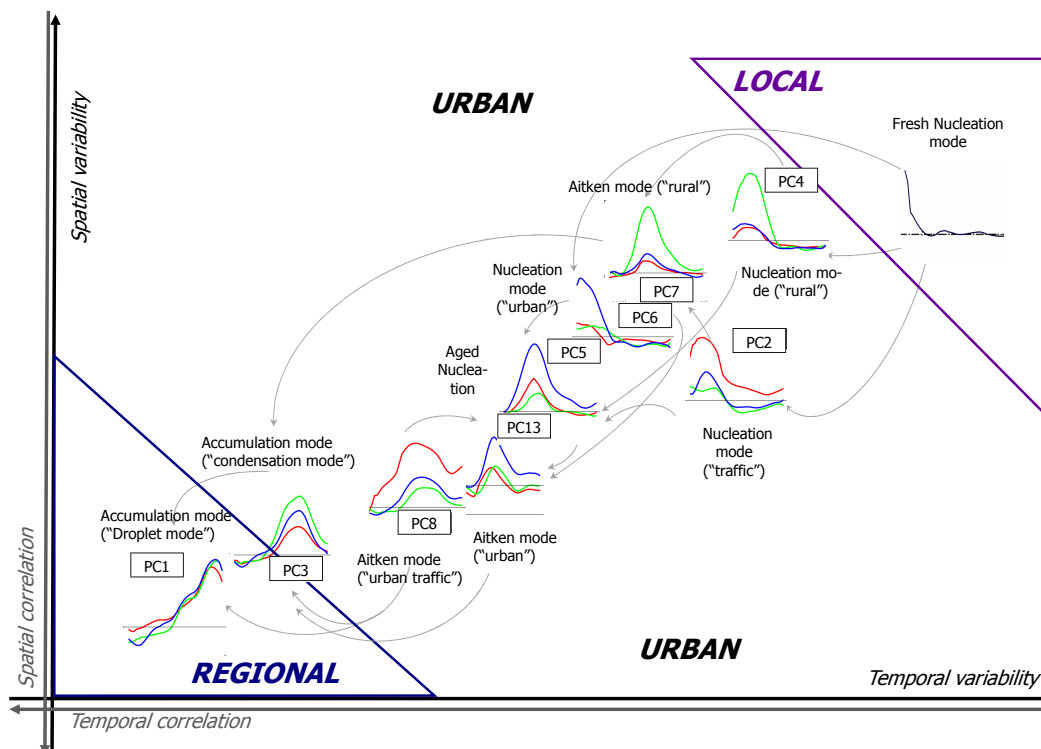


Fig. 9. Paradigm of aerosol particle modes and their evolution in space and time in the coordinate systems of variability (black axis) and correlation (grey axis). The PCs shown refer to those derived from STA3 (see Fig. 5d).

Title Page

Abstract

Introduction

Conclusions

References

Tables

Figures

◀

▶

◀

▶

Back

Close

Full Screen / Esc

Printer-friendly Version

Interactive Discussion